

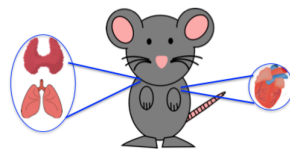
UNIVERSITY OF NAPLES FEDERICO II

DOCTORATE
MOLECULAR MEDICINE AND MEDICAL
BIOTECHNOLOGY

XXXI CYCLE



**Genetic ablation of *Hipk2* induces cardiac dysfunction
and, in combination with the loss of *Hmga1*, causes
respiratory distress and thyroid dysfunction in mice**



Tutor

Prof. Giovanna Maria Pierantoni

Candidate

Francesca Cammarota

COORDINATOR

Prof. Vittorio Enrico
Avvedimento

Academic Year 2017/2018

INDEX

ABSTRACT	1
1. INTRODUCTION	3
1.1 HIPKs protein family	3
1.2 HIPK2 structure and functions	4
1.3 HIPK2 functions	7
1.3.1 Role of HIPK2 in kidney fibrosis	7
1.3.2 Role of HIPK2 in neurological diseases	8
1.3.3 Role of HIPK2 in cancer	10
1.4 HIPK2 Knock-out mouse models	11
1.5 HMGA proteins	12
1.6 HMGA expression in growth and development	14
2. AIMS OF THE STUDY	16
3. MATERIALS AND METHODS	17
3.1 Cell culture and transfections	17
3.2 RNA extraction, RT-PCR and Quantitative real time RT-PCR	17
3.3 Western blotting and antibodies	19
3.4 Animals	19
3.5 Echocardiography	20
3.6 Wheat germ agglutinin (WGA) and histoenzymatic staining	21
3.7 Fluorescence microscopy	22
3.8 Statistical analysis	22
4. RESULTS	23
4.1 Loss of HIPK2 induces cardiac dysfunction in mice	23
4.2 Loss of HIPK2 induces an increase of the size of cardiomyocytes, cardiac inflammation and fibrosis	25
4.3 Expression levels of cardiac failure markers are increased in HIPK2-KO mice	27
4.4 Altered autophagic pathway in HIPK2-KO mice	28
4.5 HIPK2 protein levels increase during differentiation of cardiomyoblasts	30
4.6 DKO mice show respiratory failure at birth and a decrease of expression of surfactant proteins in lung	34
4.7 DKO mice display thyroid dysfunction	37
5. DISCUSSION AND CONCLUSIONS	41
6. DECLARATION	45

7. REFERENCES	46
8. LIST OF PUBLICATIONS	54

ABSTRACT

The Homeodomain-interacting protein kinase 2 (HIPK2) is a nuclear serine–threonine kinase able to interact with homeobox proteins and other transcription factors. It is a sensor for various extracellular stimuli thus regulating several signal pathways such as apoptosis, embryonic development, DNA-damage response, and cellular proliferation. As consequence, HIPK2 alterations are involved in diseases such as cancer and fibrosis. HIPK2 knock-out (KO) mice have been generated and display a reduction in body size compared to WT mice and severe psychomotor behavioral abnormalities (such as dystonia, impaired coordination, reduced motility, claspings of their posterior limbs when suspended by tails and reduced responses to novelty) that are consistent with cerebellar defects. In this thesis, we have further investigated the *in vivo* role of HIPK2 analyzing other phenotypic features of the HIPK2-KO mice.

Firstly, we investigated the cardiac phenotype consequent to the kinase depletion. Echocardiographic analysis performed on HIPK2-KO mice at 4 and 12 months showed a significant reduction in systolic function in the adulthood, by a left ventricle fractional shortening (LVFS), and an increased in left ventricular (LV) mass/body weight (BW) ratio in HIPK2-KO mice in comparison with wild-type (WT) littermates. Consistently, increased expression levels of cardiac failure hallmarks, such atrial and brain natriuretic peptides, ANP, BNP, and myosin heavy chain, β -MHC were observed. In addition, the histological analysis of the myocardium was performed by WGA staining of cardiac sections at different age (4, 6, 12 and 18 months of age), revealing areas of fibrosis, mild inflammatory infiltrate and sarcoplasmic red deposits. At cellular level, a lot of p62/SQSTM1-positive autophagic vacuoles were observed in sections of hearts from KO mice at 18 months of age. In order to investigate the molecular mechanisms by which HIPK2 depletion causes cardiac failure, H9C2 rat cardiomyoblasts have been stably silenced for *HIPK2* gene expression through a doxycycline-inducible system. HIPK2-depleted clones showed a strong upregulation of ANP, BNP and β -MHC markers with respect to control ones, thus representing a good model to study the phenotype observed in KO mice.

As HIPK2 protein interacts with the architectural chromatin protein HMGA1 (Pierantoni et al. 2001), *Hmgal/Hipk2* double knock-out mice (DKO) have been generated in our laboratory, crossing *Hmgal*-KO (A1-KO) mice and *Hipk2*-KO mice, in order to understand the functional role of *Hmgal* and *Hipk2* complex *in vivo*. High Mobility Group A1 (HMGA1) is an architectural chromatin protein whose overexpression is a feature of malignant neoplasia with a causal role in cancer initiation and progression. HIPK2 and HMGA1 proteins physically interact, and HIPK2 phosphorylates HMGA1 modulating its DNA binding capacity. We observed that the 50% of DKO newborn mice dies within one day of life (P1) and autoptic examination showed that lung phenotype was characterized by collapsed immature sac-like alveoli and unexpanded alveolar spaces. Through molecular analysis, we have demonstrated that HMGA1 and HIPK2 positively regulate surfactant protein expression, since DKO mice show a strongly decreased expression of surfactant genes, both during embryogenesis and at birth. Surfactant proteins are components of lung surfactant which is essential for several lung functions. In addition, autoptic examination of DKO mice at P1 revealed also thyroid abnormalities represented by irregular structures of thyroid follicles devoid of colloid. Immunohistochemistry (IHC) and molecular analysis of thyroid late differentiation markers on DKO thyroid glands showed a reduction of expression levels of Thyroglobulin (*Tg*), Tireoperoxidase (*Tpo*) and Thyrotropin receptor (*Tshr*) DKO mice compared to control mice at P1. The expression of transcription factors required for the expression of the thyroid specific differentiation markers, FOXE1, PAX8 and TTF-1 were strongly reduced in thyroids from DKO at P1 (Gerlini et al. Manuscript in submission). Altogether these data suggest that the lack of both *Hmgal* and *Hipk2* genes impairs the expression of PAX8 and FOXE1 in thyroid gland and, consequently, of thyroid differentiation markers, indicating that HMGA1/HIPK2 interaction is crucial also for thyroid development.

1. INTRODUCTION

1.1 HIPKs protein family

The evolutionary conserved family of homeodomain-interacting protein kinases (HIPKs) has been identified at the end of '90s by a yeast two hybrid screening as interactors of NK homeoproteins and consists of four related kinases, from HIPK1 to HIPK4 (Kim et al. 1998). HIPKs are involved in several cellular processes such as proliferation, cell differentiation and apoptosis (D'Orazi et al. 2002; Hofmann et al. 2002). All HIPK proteins are nuclear serine/threonine kinases localized in the nuclear speckles, but a small fraction of these proteins is found also in the nucleoplasm or cytosol (D'Orazi et al. 2002; Hofmann et al. 2002; Rinaldo et al. 2007). They are characterized by a strong sequence homology among them: 90% in kinase domain, 70% in homeobox-interacting domain and 65% in C terminal region (Kim et al. 1998). The high sequence homology among HIPK1, HIPK2 and HIPK3 proteins suggests that they may be functionally redundant. This seems to be confirmed by the phenotype of HIPK1 and HIPK2 Knock-Out (KO) mice: single *Hipk1* or *Hipk2*-KOs are viable (Kondo et al. 2003; Wiggins et al. 2004), whereas the double KO *Hipk1/Hipk2* embryos die before birth, with various anomalies of the hematopoiesis and defects in blood vessel formation (Isono et al. 2006; Rinaldo et al. 2007).

Recently, new functions related to the kinase activity of these proteins have been discovered. HIPK1 and HIPK2 have been found to phosphorylate and inhibit the carbon catabolite repressor 4 (CCR4)-negative on TATA (NOT), a regulator of the major steps of the mRNA metabolism (Gil et al. 2016). An important role in insulin secretion and in the pathogenesis of diabetes is emerging for HIPK3 (Shojima et al. 2012) and HIPK3 contributes to the pathogenesis of Huntington's disease (HD). HD is caused by accumulation in neurons of mutant HTT protein (mHTT) with an expanded polyglutamine tract (polyQ); the accumulation is increased by defective autophagy. Indeed, HIPK3 has been identified as a positive regulator of mHTT because of its ability to inhibit autophagy (Fu et al. 2018). HIPK4 has been identified as an inhibitor of human epithelial cell differentiation, as its knock-down during the epithelial-differentiation of induced pluripotent stem cell (iPSCs)

increases the amount of skin epithelial precursors (Larribère et al. 2017).

1.2 HIPK2 structure and functions

The best characterized member of the family is HIPK2, which is structurally characterized by a SUMOylation site at lysine 25, a Ser/Thr kinase domain, a protein–protein interaction region, called Homeobox-interacting domain, a region rich in proline (P), glutamic acid (E), serine (S) and threonine (T) that act a signal peptide for protein degradation (PEST region), a speckle-retention signal essential for the subcellular localization in nuclear bodies (NBs) and an auto-inhibitory domain (AID) (Fig. 1). Indeed, HIPK2 activity is modulated by several post-translational modifications. The ubiquitination provides the addition of a small protein of ubiquitin at a lysine of the target protein and subsequently, on a lysine of ubiquitin. The E3 ubiquitin ligase MDM2 catalyzes this reaction at the residue K1182 of HIPK2, located in the auto-inhibitory domain (AID) (Rinaldo et al. 2007b). Ubiquitination has been associated with the inactivation of HIPK2; sumoylation at lysine 25, on the other hand, is related to both HIPK2 activation and activity. In particular, following DNA damage, HIPK2 phosphorylates its E3 SUMO ligase Pc2 that enhances HIPK2 ability to act as a transcriptional repressor (Roscic et al. 2006).

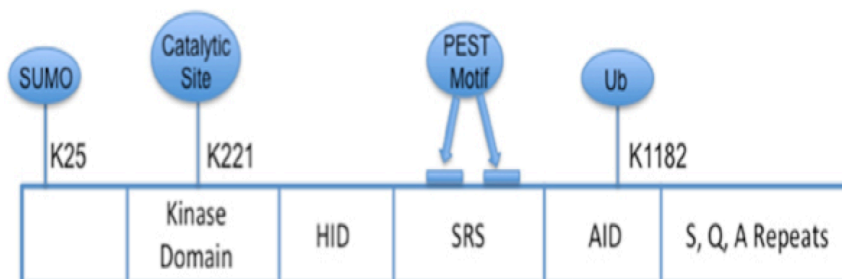


Figure 1. Schematic representation of HIPK2 protein structure. Functional domains and important residues of HIPK2 protein are shown. K25: sumoylation site; K221: catalytic site; HID: homeobox-interacting domain; SRS: speckle-retention signal; AID: auto-inhibitory domain; K1182: ubiquitination site (Adapted from Nugent et al. 2015).

HIPK2 kinase activity depends on the aminoacid K221 involved in ATP binding, which is highly conserved (Kuwano et al. 2016). The importance of the lysine has been confirmed by substitution with an arginine or an alanine that leads to the loss of the kinase activity: the mutant protein K221R (kinase dead, KD) keeps the ability to interact with its target proteins, but it is unable to phosphorylate both target protein and itself (D’Orazi et al. 2002; Hofmann et al. 2002). The kinase activity is important also for its nuclear bodies (NB) association, since HIPK2 KD shows a pan-nuclear distribution.

HIPK2 plays a dual role in transcriptional regulation as it can repress or activate the transcription of many promoters. At first HIPK2 was identified as a transcriptional regulator and a corepressor for homeobox proteins. The repressive function relies on its ability to bind general transcriptional regulators, including methyl-DNA-binding proteins histone acetyltransferase p300 (p300), p53 and cAMP response element-binding protein-binding protein (CBP) (Fig. 2) (D’Orazi et al. 2002; Hofmann et al. 2002; Rinaldo et al. 2007).

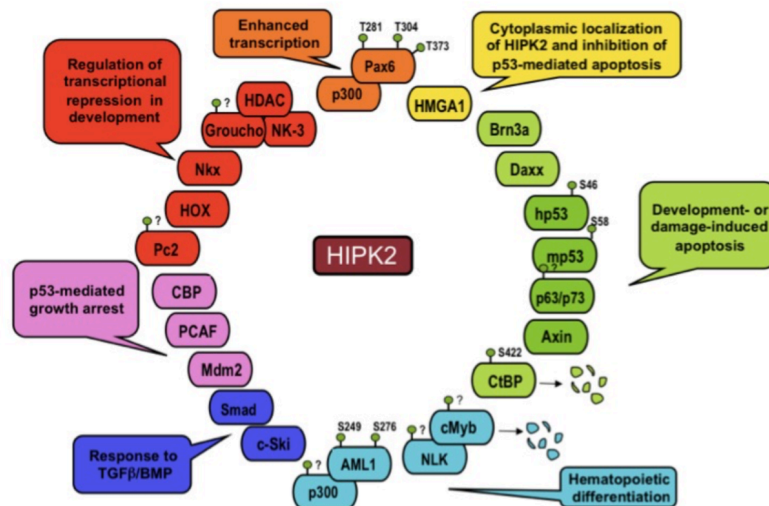


Figure 2. HIPK2 interactors. Schematic representation of HIPK2 interactors (Adapted from Rinaldo et al. 2007).

HIPK2 activating function depends on its ability to phosphorylate transcription factors, such as p53 (D’Orazi et al. 2002; Fusco and Fedele, 2007; Hofmann et al. 2002; Rinaldo et al. 2007) and activate

transcription factor 1 (ATF1) (Hailemariam et al. 2010). Thanks to the identification of its interactors, several studies have highlighted the importance of HIPK2 in different biological processes, such as embryonic development, proliferation and apoptosis. Moreover, in response to severe DNA damage, HIPK2 activates the apoptotic pathway by interacting and phosphorylating p53 at Ser46 (D'Orazi et al. 2002; Fusco and Fedele, 2007; Hofmann et al. 2002; Rinaldo et al. 2007). Indeed, in normal condition, p53 has a short half-life due to the binding with MDM2, an E3-ubiquitin ligase that induces p53 proteosomal degradation. After severe genotoxic stress, HIPK2 phosphorylates itself and p53, allowing it to break away from MDM2 and to accumulate in the nucleus. Here, p53 activates the transcription of pro-apoptotic genes as *Bax* and *PIG3* and downregulates *p21^{Waf1}* (Di Stefano et al. 2005).

However, HIPK2 regulates apoptosis also by p53-independent pathways. Indeed, HIPK2 can bind and phosphorylate the anti-apoptotic factor transcription corepressor C-terminal Binding Protein (CtBP), inducing its degradation and sensitizing cells to apoptosis (Zhang et al. 2003). HIPK2 is also involved in the control of cell growth, as demonstrated from studies conducted on HIPK2-KO cells. Mouse embryonic fibroblasts (MEF) isolated from *Hipk2-KO* mice show a significant reduction in proliferation compared to WT counterparts (Iacovelli et al. 2009).

Because of its ability to modulate the above mentioned cellular processes, HIPK2 is involved in the pathogenesis of important human diseases, including cancer, fibrosis and neurological diseases.

Indeed, HIPK2 is also functionally related to the TGF- β and MeCP-2 pathways. It can bind the transcriptional activators Smad1-4, involved in TGF- β pathway through the homeobox-interacting domain. HIPK2 expression is upregulated by TGF- β 1 treatment in hepatic stellate cells (HSCs) and in liver fibrotic tissue. Furthermore, knock-down of HIPK2 inhibits TGF- β 1 induced HSCs proliferation and decreases the expression of fibrosis markers, thus suggesting that HIPK2 may be a potential target for the treatment of liver fibrosis (He et al. 2017). HIPK2 has also been identified as regulator of methyl-CpG binding protein 2 (MeCP2) protein stability. MeCP2 levels are altered in several neurological diseases such as autistic behavior, and genetic mutations that alters MeCP2 levels are also responsible for Rett syndrome (caused by loss-of-function mutations). The discovery of druggable MeCP2 regulators, such as

HIPK2, may uncover new therapeutic approaches for these diseases (Lombardi et al. 2017).

In addition, as previously mentioned, HIPK2 can bind and phosphorylate architectural transcription factors, including the High Mobility Group A1 (HMGA1) proteins. Several studies show that HMGA1 and HIPK2 share various fields of interactions, such as regulation of cell proliferation, apoptosis, and regulation of p53 activity. Indeed, HIPK2 phosphorylates HMGA1a at Ser-35, Thr-52, and Thr-77 residues and its isoform HMGA1b at the corresponding sites Thr-41 and Thr-66, decreasing their binding affinity to DNA and altering the HMGA1-mediated regulation of gene expression (Zhang et al. 2007). Indeed, while HMGA1 is able to antagonize p53-driven transcription of apoptosis-related genes, HIPK2 is able to potentiate p53 pro-apoptotic activity by phosphorylating it at Serine 46 residue. Furthermore, HMGA1, HIPK2 and p53 form a multiprotein complex with the transcription factor Brn-3a involved in the regulation of the expression of the *Bcl2* anti-apoptotic gene (D'Orazi et al. 2002; Fusco and Fedele, 2007; Hofmann et al. 2002; Rinaldo et al. 2007).

1.3 HIPK2 functions

1.3.1 Role of HIPK2 in kidney fibrosis

Renal fibrosis occurs in response to tissue injury: the effort to repair damage begins with the recruitment of inflammatory cells and with the activation of matrix producing cells that leads to tubular cell apoptosis and loss of renal function (Nugent et al. 2015). HIPK2 has been identified as a master regulator of kidney fibrosis in renal tubular epithelial cells (RTEC) infected with HIV. In fact, HIPK2 induces expression of pro-fibrosis and apoptosis markers in RTEC, likely due to its role in activating p53, TGF- β , and Wnt/Notch pathways (Fig. 3).

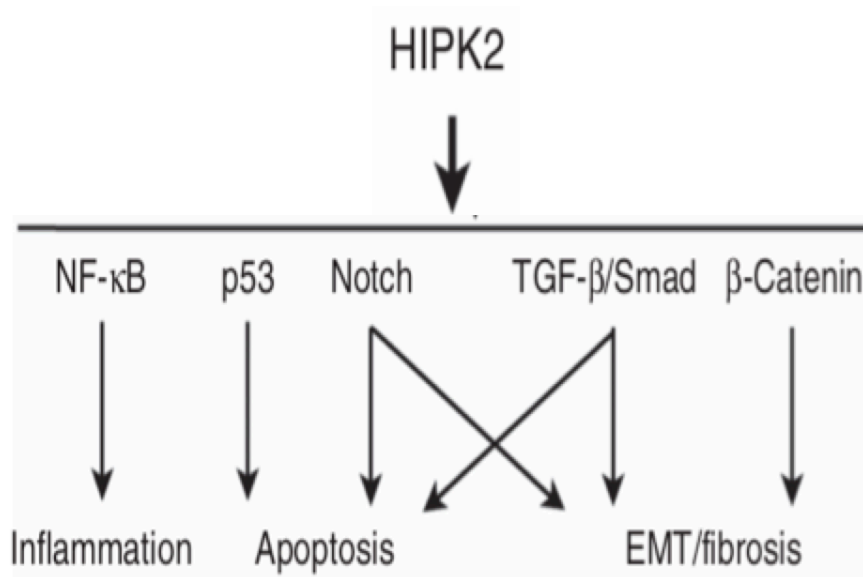


Figure 3. HIPK2 mediated signaling pathways. HIPK2 activates multiple downstream signaling pathways including p53-mediated DNA damage signaling pathways, TGF- β /Smad, Wnt/ β -catenin, Notch and NF- κ B pathways to regulate cell growth, apoptosis, and development (Adapted from Fan et al. 2014).

However, suppression of HIPK2 activity prevents TGF- β mediated induction of fibrosis markers and attenuate apoptosis (Nugent et al. 2015). Indeed, HIPK2 levels can be regulated through seven in absentia homolog-1 (SIAH-1) mediated proteasomal degradation. This involves an accumulation of HIPK2 and a consequent development of fibrosis (Nugent et al. 2015). In this scenario, HIPK2 could be a new therapeutic target for kidney disease.

1.3.2 Role of HIPK2 in neurological diseases

HIPK2 plays an important role in the development of neurological diseases (Fig. 4). Firstly, Doxakis et al. reported BAX- and HIPK2- in sensory and sympathetic neurons in response to neurotrophin deprivation (Doxakis et al. 2004). The expression of HIPK2 in dopaminergic neurons is required for TGF-mediated survival during programmed cell death. In fact, HIPK2-KO mice show a severe neurodegenerative Parkinson-like phenotype, characterized by the selective through apoptotic processes of the dopaminergic neurons of

the grey substance. In this context, HIPK2 acts on the TGF β signaling pathway through the interaction with the transcription factor Smad3, independently from its kinase activity (Zhang et al. 2007). These results suggest a role of HIPK2 as a survival factor in dopaminergic neurons. Indeed, in our lab, it has been characterized the expression level of HIPK2 in brain cortex, hippocampus, striatum and cerebellum from mice, founding that HIPK2 level progressively decreases with age in brain cortex, hippocampus and striatum, whereas increases in the cerebellum (Anzilotti et al. 2015). Indeed, in cerebellar Purkinje cells, lack of HIPK2 expression negatively interferes with Wnt/ β -catenin function, giving rise to an impaired degradation of β -catenin (Kim et al. 2010), a hallmark of Parkinson's disease, spinocerebellar ataxia, and other neurodegenerative diseases. Mice lacking HIPK2 display atrophic lobules and smaller cerebellum and a strong reduction in cerebellar Purkinje neurons during adulthood (Anzilotti et al. 2015). Moreover, HIPK2-KO mice display severe psychomotor behavioral abnormalities consistent with cerebellar defects, such as dystonia, impaired coordination, reduced motility, and claspings of posterior limbs of mice when suspended by the tails (Zhang et al. 2007). Therefore, HIPK2 may be considered a potential therapeutic target for treating some forms of cerebellar ataxia.

Furthermore, the neuronal dysfunction and death at the base of many neurodegenerative diseases are associated with the accumulation of abnormally folded proteins. In particular, the alteration of protein homeostasis through the impairment of the ubiquitin-proteasome pathway could play a critical role in the pathogenesis of amyotrophic lateral sclerosis (ALS) and contribute significantly to the progression of the disease. Recently it has been demonstrated that HIPK2 is a possible link between stress and cell death necessary and sufficient to promote endoplasmic reticulum-mediated stress cell death (UPR^{RE}) (Lee et al. 2016) .

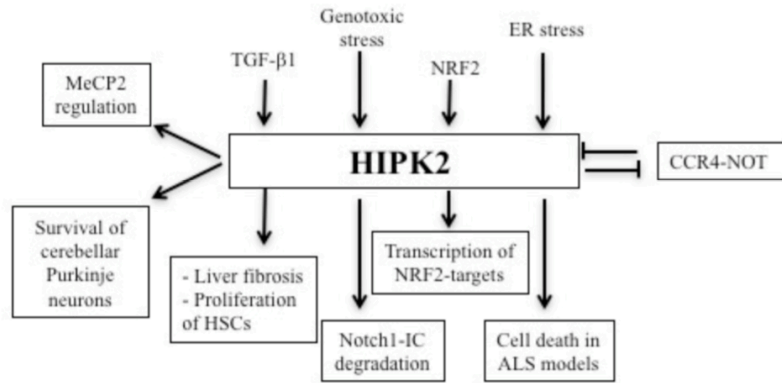


Figure 4. Schematic representation of the recent findings about HIPK2 regulation and functions (Image from Conte et al. 2018).

1.3.3 Role of HIPK2 in cancer

Many evidences demonstrate that HIPK2 plays an important role in cancer. HIPK2 can be activated by several types of genotoxic damages, including ultraviolet radiation (UV), or ionizing radiation (IR), and its expression is triggered by antitumor drugs such as cisplatin (D’Orazi et al. 2002). HIPK2 role in cancer is based above all through the regulation of important molecules involved in cancer, among them the most important is p53. HIPK2 phosphorylates p53 at Serine 46 (Ser46) and allows recruitment of histone acetylase (HAT) p300 for efficient p53 acetylation at lysine 382 (Lys382), thus inducing an increase of p53 stability (Hofmann et al. 2002). Interestingly, p53 activation induces caspase-6 which is responsible for caspase-mediated HIPK2 cleavage at positions 916 and 977 (Gresko et al. 2006). This C-terminus truncated HIPK2 results in a hyperactive kinase which potentiates p53Ser46 phosphorylation and activation of apoptosis (Gresko et al. 2006).

Other studies have demonstrated that HIPK2 phosphorylates β -catenin inducing its proteasomal degradation, thus interfering with the transcription of several β -catenin target genes, including Vascular Endothelial Growth Factor (VEGF) involved in tumor angiogenesis and tumor growth (Puca et al. 2008).

Moreover, HIPK2 expression is decreased in breast, thyroid and colon carcinomas, as demonstrated by RT-PCR analysis and genetic loss at HIPK2 locus 7q32-34 was found by loss of heterozygosity

(LOH) analysis in thyroid cancer cells. Therefore, HIPK2 inhibitions do exist in tumors and depend by several mechanisms including HIPK2 cytoplasmic localization, protein degradation, and loss of heterozygosity (LOH) (Lavra et al. 2011; Pierantoni et al. 2002).

Hipk2 is a haploinsufficient tumor suppressor gene *in vivo*, showing loss of one *Hipk2* allele in 30 % of the tumors and increased susceptibility of *Hipk2*^{+/-} mice to radiation-induced thymic lymphoma (Mao et al. 2011).

Few mutations of HIPK2 gene have been identified in human acute myeloid leukemias (AMLs), leading to an aberrant HIPK2 nuclear distribution inducing an impairment of p53 apoptotic transcriptional activity (Li et al. 2007).

Altogether, these findings highlights the role of HIPK2 as tumor suppressor that is in line with the outcome of genetic HIPK2 deletion in mice where *Hipk2*^{-/-} and *Hipk2*^{+/-} mice are tumor prone and undergo to skin carcinogenesis by the two stage carcinogenesis protocol (Wei et al. 2007). However, HIPK2 amplification has been detected in pilocytic astrocytomas and its overexpression in a glioma cell line has been resulted in an increased proliferation rate (Yu et al. 2009). In this scenario, we can say that HIPK2 has an important and complex role in cell proliferation, which is not easy to define. In fact both the loss and the gain of function of HIPK2 could promote cell proliferation. Therefore these studies have to be better defined and need to further investigations.

1.4 HIPK2 Knock-out mouse models

Several *Hipk2*-KO mice have been generated by several groups. Single *Hipk2*-KO mice show a reduction in body size, associated with severe psychomotor behavioral abnormalities consistent with cerebellar defects, such as dystonia, impaired coordination, reduced motility, and claspings of posterior limbs of mice were suspended by their tails, consistent failure to finish the tandem walk, poor motor coordination, and reduced responses to novelty (Anzilotti et al. 2015) (Fig. 5).

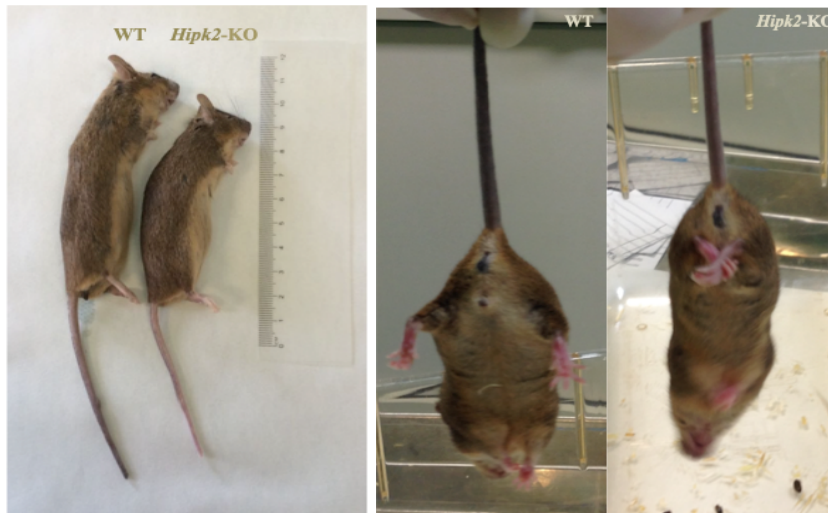


Figure 5. *Hipk2*-KO mice phenotype. Left *Hipk2*-KO mice were smaller than WT. Middle WT mice after suspension by the tail. Right *Hipk2*-KO mice showed a reduced motility in their posterior limbs after suspension by their tails.

Moreover, HIPK2-null mice are characterized by head and snout crushed, a curvature of the spine, and distortion of the front and rear legs (Anzilotti et al. 2015). Although these phenotypes, single *Hipk2*-KO are viable and fertile. HIPK2-KO mice show cerebellum lobular atrophy and Purkinje cell apoptosis because of the activation of an apoptotic process associated with a compromised ubiquitin-mediated proteasomal degradation pathways (Anzilotti et al. 2015).

Moreover, *Hipk1*^{-/-} *Hipk2*^{-/-} double-mutants were generated from Isono et al. These embryos were lost between E9.5 and E12.5 exhibiting neural tube closure defect (NTD) and exencephaly. These defects are due to a reduction in proliferation rate of cells of the neural tube and the cephalic mesoderm. Therefore, *Hipk1* and *Hipk2* act in synergy to mediate growth regulation upon morphogenetic signals, although *Hipk2* may exert a slightly dominant role (Isono et al. 2006).

1.5 HMGA proteins

The crucial role exerted by HIPK2 in many biological processes, from apoptosis to cell proliferation, is mostly due to its ability to bind and phosphorylate several chromatin modifiers and

transcription factors acting, thus acting as coactivator or corepressor depending on cellular context. The nuclear non-histone chromatin High Mobility Group A1 (HMGA1) protein represents an important architectural chromatin protein that interacts with HIPK2 (Pierantoni et al. 2001). The HMG proteins represent the largest group of non-histone chromatin components (Bustin and Reeves, 1996), characterized by an enrichment in both acidic and basic (charged) amino acids. All HMG proteins are involved in modulating nucleosome and chromatin structure in different nuclear activities such as transcription, replication and DNA repair (Reeves et al. 2010). In mammals HMG proteins have been classified into three families: HMGA, HMGB and HMGN, that are distinguished from each other by their DNA-binding motifs.

The HMGA protein family is composed of two subfamilies, HMGA1 and HMGA2. The first subfamily consists of three proteins (HMGA1a, HMGA1b and HMGA1c) produced by the translation of alternatively spliced transcript derived from a single gene. The second subfamily contains only one protein (HMGA2) encoded by a different gene. All HMGA proteins contains three “AT-hook” domains, except for the HMGA1c variant which contains only two domains, and a C-terminal domain involved in protein-protein interaction (Reeves, 2010) (Fig. 6).

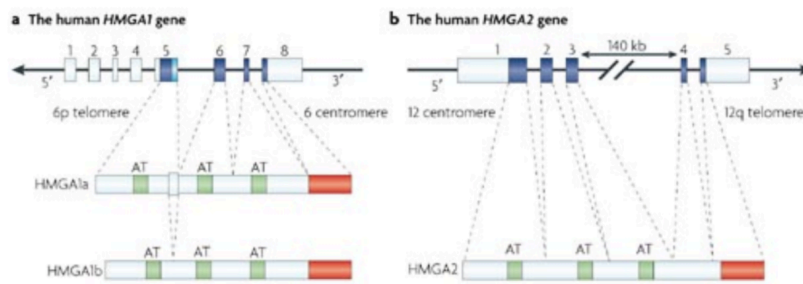


Figure 6. Schematic representation of HMGA1 and HMGA2 genes and proteins. Each proteins contains three basic domains, called AT hook (green box), with which they bind DNA, and an acidic carboxy-terminal region (red box) involved in protein-protein interactions (Image from Fusco and Fedele, 2007).

Through these domains, HMGA proteins can bind to chromatin and proteins in a reversible way and regulate gene expression positively or negatively. These proteins can be modified through different post-

translational modifications (PTMs) which control the interaction with DNA and other proteins influencing their biological activities. The PTMs include lysine acetylation, arginine/lysine methylation, serine/threonine phosphorylation and ADP-ribosylation (Sgarra et al. 2008). HIPK2 can phosphorylate HMGA1 at Ser-35, Thr-52 and Thr-77. These HIPK2-mediated phosphorylations decrease HMGA1 binding affinity toward DNA (Zhang et al. 2007), thus inducing an inhibitory effect on cell growth at the G2/M phase of the cell cycle (Pierantoni et al. 2001).

1.6 HMGA expression in growth and development

The *HMGA* genes are expressed at low level in normal adult tissues, whereas they are expressed at high level in all embryonic tissues (Chiappetta et al. 1996) and in malignant cells both *in vivo* and *in vitro* (Fusco and Fedele, 2007). Indeed, HMGA1 and HMGA2 are expressed at high levels in all tissues in the early stages of embryogenesis. The expression becomes restricted to specific organs in the later stage of development until to disappear (Bustin and Reeves, 1996).

HMGA1 and HMGA2 proteins play an important role in embryonic development, adipocytic cell growth and differentiation. The disruption of the *HMGA1* and *HMGA2* genes induces an altered phenotype (Federico et al. 2014; Zhou et al. 1995). HMGA1 KO mice show a comparable or a slightly less body weight, and display an increased ventricular mass and ventricular wall thickness (Federico et al. 2014). The *Hmga1*-null mice exhibit a comparable size to the WT littermates, whereas the *Hmga2*-KO mice show a pygmy phenotype. Indeed fat tissue is drastically reduced in *Hmga2*-null mice, whereas it does not seem to be modified in *Hmga1*-null mice (Zhou et al. 1995). Therefore the phenotype of the *Hmga1*-KO mice and the *Hmga2*-KO mice indicates that these genes exert also distinct functions.

Therefore many genes are regulated by both HMGA proteins and several functions controlled by one of them are compensated by the other family member. To better investigate the role of these genes in development, *Hmga1/Hmga2*-null mice were generated. These mice display a more severe phenotype, characterized by a reduced vitality due to high rate of death in utero. *Hmga1/Hmga2*-null mice show very small size, even lower than that of the single *Hmga2*-KO mice, so they are called “superpygmy”. This phenotype depends on a lower

growth rate due to a decreased expression of cyclin A and cyclin E and a decreased activity of E2F1 (Federico et al. 2014).

2. AIMS OF THE STUDY

As previously discussed, *Hipk2* is widely expressed in both embryonic and adult tissues, suggesting that this gene may have an important role in the development and/or in the homeostasis of several organs. To better define the role of HIPK2 *in vivo*, the aim of my thesis was to further characterize the effects of the HIPK2 expression loss, alone or in combination with the loss of its interactor HMGA1, through the phenotypic analysis of both *Hipk2*-KO mice and HMGA1/HIPK2 double KO mice. Histological examination and immunohistochemical analysis of several organs isolated from *Hipk2*-KO mice have suggested a crucial role of HIPK2 in cardiac homeostasis. Therefore we evaluated the role of HIPK2 in cardiac function through immunohistochemistry, echocardiography and Western blot analysis.

Moreover, to understand the role of HMGA1/HIPK2 functional interaction *in vivo*, we generate mice carrying the disruption of both the *Hmgal* and *Hipk2* genes by crossing the HMGA1-KO (Federico et al. 2014) with the HIPK2-KO mice (Anzilotti et al. 2015; Rinaldo et al. 2012). About 50% of these mice die within 12 hours from the birth for respiratory failure, whereas the remaining survive and appear smaller than WT counterparts. For these reasons, we performed histological examination of DKO lungs and thyroid, and evaluated if HMGA1/HIPK2 complex is able to regulate the expression of the crucial markers involved specifically in the differentiation of lung and thyroid.

3. MATERIALS AND METHODS

3.1 Cell culture and transfections

H9C2 rat cardiomyoblasts (CRL-1446, ATCC, Manassas, Virginia) were cultured in Dulbecco's Minimal Essential Medium (DMEM), low Glucose (1 g/l), 2 mM-glutamine, 1 mM sodium pyruvate, supplemented with 10% FBS, and 10% penicillin-streptomycin, at 37 °C in a humidified 5% CO₂ atmosphere. For the differentiation in cardiomyocytes, the percentage of FBS was decreased from 10% to 1%. For stable transfections, H9C2 cardiomyoblasts were plated at a density of 5×10^5 cells/100-mm tissue culture dish in antibiotic-free DMEM containing 10% FBS, and incubated for 24 h at 37 °C with 5% CO₂. 60–70% confluent cells were transfected using IBAfect reagent, according to the manufacturer's instructions, with a plasmid carrying shRNA (pINDUCER HIPK2 sh-HIPK2, kindly provided by Prof. ML Schmitz, University of Gießen, Germany) targeting HIPK2 or with a control plasmid encoding a non-targeting shRNA (pINDUCER luciferase sh-CTR, kindly provided by Prof. ML Schmitz). Forty-eight hours later, cells were selected in the presence of 0.3 µg/ml of puromycin. After 10 days from selection, the pools clones were treated with 1 µg/ml of doxycycline and screened to verify the silencing of HIPK2.

3.2 RNA extraction, RT-PCR and Quantitative real time RT-PCR

Total RNAs from H9C2 stable pool clones were extracted using Trizol reagent following the manufacturer's instruction. Five hundred nanograms of RNA were reverse transcribed for cDNA synthesis with Iscript RT-PCR system (Biorad Laboratories). Reverse transcription of the RNAs was followed by quantitative real-time PCR (q-PCR) performed with the SYBR Green real-time PCR master mix kit (FS Universal SYBR Green MasterRox/Roche Applied Science). The reactions were visualized by SYBR Green analysis (Applied Biosystem Inc, Foster City, CA, USA) on CFX96 Touch™ instrument (Biorad Laboratories). Primers used for gene analysis were:

rat ANP-Forward: 5'-CTTCTTCCTCTTCCTGGCCT-3'

rat ANP-Reverse: 5'-TTCATCGGTCTGCTCGCTCA-3'

rat BNP-Forward: 5'-TCCTTAATCTGTCGCCGCTG-3'
 rat BNP-Reverse: 5'-AGGCGCTGTCTTGAGACCTA-3'
 rat β -MHC- Forward: 5'-CTGACTGAACAGCTGGGCTC-3'
 rat β -MHC- Reverse: 5'-AACTCTGGAGGCTCTTCACT-3'
 mouse/rat S18-Forward: 5'-AAACGGCTACCACATCCAAG-3'
 mouse/rat S18-Reverse: 5'-CCTCCAATGGATCCTCGTTAA-3'
 rat/mouse HIPK2-Forward: 5'-CCACATGTCAATTGCCTCAC-3'
 rat/mouseHIPK2-Reverse:5'-AGGTCATCGACTTTGGTTCAG-3'
 rat MLC2V-Forward: 5'-GACCCAGATCCAGGAGTTCAAGG-3'
 rat MLC2V-Reverse: 5'-CGAGGGCAGCAAACGTGTCCC-3'
 Total RNA was extracted also from several samples of cardiac apex of left ventricle (LV) obtained from the whole frozen hearts of mice at 12 months of age and from DKO thyroid and lungs, using the TRIzol (Invitrogen) according to the manufacturer's instruction. The protocol of cDNA synthesis and qPCR are the same for the cells. The primers used were:
 mouse β -MHC- Forward: 5'-CGGAAACTGAAAACGGAAAG-3'
 mouse β -MHC- Reverse: 5'-TCCTCGATCTTGTCGAACTTG-3'
 mouse ANP-Forward: 5'-CACAGATCTGATGGATTTCAAGA-3'
 mouse ANP- Reverse: 5'-CCTCATCTTCTACCGGCATC-3'
 mouse BNP- Forward: 5'-GTCAGTCGTTTGGGCTGTAAC-3',
 mouse BNP- Reverse: 5'-AGACCCAGGCAGAGTCAGAA-3'
 mouse Sp-A- Forward: 5'-CTGGAGAACATGGAGACAAGG-3'
 mouse Sp-A- Reverse: 5'-AAGCTCCTCATCCAGGTAAGC-3'
 mouse Sp-B- Forward: 5'-AACCCACACCTCTGAGAAC-3'
 mouse Sp-B- Reverse: 5'-GTGCAGGCTGAGGCTTGT-3'
 mouse Sp-C- Forward: 5'-GGTCCTGATGGAGAGTCCAC-3'
 mouse Sp-C- Reverse: 5'-GATGAGAAGGCGTTTGAGGT-3'
 mouse-*Tg*-Fw 5'-CATGGAATCTAATGCCAAGAACTG-3'
 mouse-*Tg*-Re 5'-TCCCTGTGAGCTTTTGGAAATG-3'
 mouse-*Tpo*-Fw 5'-CAAAGGCTGGAACCCTAATTTCT-3'
 mouse-*Tpo*-Re 5'-AACTTGAATGAGGTGCCTTGTCA-3'
 mouse-*Tshr*-Fw 5'-TCCCTGAAAACGCATTCCA-3'
 mouse-*Tshr*-Re 5'-GCATCCAGCTTTGTTCCATTG-3'
 mouse Actin-Forward: 5'-CTAAGGCCAACCGTGAAAAG-3'
 mouse Actin-Reverse: 5'-ACCAGAGGCATACAGGGACA-3'
 All standards and samples were assayed in triplicate. Thermal cycling was initiated with an initial denaturation at 95 °C for 5 min. After this initial step, 40 cycles of PCR were performed.

Each PCR cycle consisted of heating at 95 °C for 30 s for melting, 55 °C for 30 s for annealing, and 72 °C for 30 s for the extension. To calculate the relative expression levels, we used the 2- $\Delta\Delta$ CT method.

3.3 Western blotting and antibodies

Cells were harvested in lysis buffer NP40 2% (20 mM Tris pH 7.5 1M, 120mM NaCl 5M, NP40 100%, 0.5 mM sodium orthovanadate, 10mM sodium fluoride, phenylmethylsulfonyl fluoride (PMSF) 1mM, aprotinin 10 μ g/ml, leupeptin 10 μ g/ml), supplemented with complete protease inhibitors mixture (Roche Branford, CT, USA). Different cardiac sections were homogenized and total protein extracts were prepared with lysis buffer NP40 2%. The lysates were incubated for 30 min in ice, and then centrifuged for 30 min at 14,000 \times rpm. Protein concentration was estimated by Bradford assay, and 80 μ g/lane of total proteins were separated on SDS gels and transferred to nitrocellulose membranes. Membranes were treated with a blocking buffer (200 mM Tris pH 7.4 2M, 9% NaCl, 0.5% Tween) containing 5% non-fat milk for 1 h at room temperature. Incubation with the primary antibody was carried out overnight at 4 °C. After washings, membranes were incubated with the HRP-conjugated secondary antibody for 1 h at room temperature. Following further washings of the membranes, chemiluminescence was generated by enhanced chemiluminescence (ECL) kit (Thermoscientific, Waltham, MA, USA). The primary antibodies used for western blotting were: anti-HIPK2 (1:100 kindly provided by Prof. ML Schmitz); anti-p62 (SQSTM1) (1:1000 MBL PM045); anti- β Actin (1:1000 sc-1615); anti γ -tubulin (1:1000, mouse monoclonal Sigma-Aldrich T6557); anti-calnexin (1:1000, Enzo ADI-SPA860-F). The secondary antibodies used were: anti-goat IgG-HRP polyclonal antibody (6160-05, Southern Biotech), goat anti-mouse IgG-HRP (sc-2005) and anti-rabbit (sc-2030).

Densitometric analyses were performed using the NIH Image software (Bethesda, MD, USA).

3.4 Animals

Hipk2-null mice were generated eliminating exon 3 of *Hipk2* gene

(coding for the entire catalytic domain) as previously described (Anzilotti et al. 2015). Mice were genotyped using the following primers to amplify either wild-type or targeted alleles:

Hipk2-Fw: 5-TAGTACCCAGGTGAACCTTGGAGT-3;

Hipk2WT-Re: 5-GCTTCTCTCAAACCTAAAGACCACGC-3;

Hipk2KO-Re: 5-CAAAGGGTCTTTGAGCACCAGA-3.

To generate *Hmgal/Hipk2* double knock-out mice (DKO), we crossed *A1-KO* mice with *K2-KO* mice, generating *Hmgal*^{+/-}/*Hipk2*^{+/-} mice, that were then mated, obtaining several combinations of *Hmgal* and *Hipk2* null alleles, including DKO. Mice were genotyped using the following primers to amplify either wild-type or targeted alleles:

mouse-*Hmgal*-Fw 5'-GGCAGACCCCAAGAAACTGG-3'

mouse-*Hmgal*-Re 5'-GGCACTGCGCAGTGGTGAT-3'

mouse-*Hipk2*-Fw 5'-GAGACACAGGCTCAAGATGG-3'

mouse-*Hipk2*-Re 5'-TCTGCTCGTAAGGTAGGCTT-3'

The mice included in the study were housed with no more than 5 per cage, maintained under identical conditions of temperature (21±1°C), humidity (60±5%) and light/dark cycle, and had free access to normal mouse chow. Experiments were performed according to the international guidelines for animal research. The experimental protocol was approved by the Animal Care Committee of the "Federico II" University of Naples.

3.5 Echocardiography

For ultrasound echocardiographic studies, mice (WT, n=15 and HIPK2-KO, n=15) at different ages (4, 6 and 12 months) were analyzed. Echocardiography is a useful non-invasive method to visualize the cardiovascular structures and evaluate cardiac function in mice with a 30-MHz RMV-707B scanning head. Just before the acquisition of the echo images, the mice were anesthetized with an intraperitoneal (i.p.) injection of Tiletamine 5 ml/kg, Zolazepam 5 ml/kg (Zoletil 100) and Xylazine 5 mg/Kg (Sigma-Aldrich) in order to minimize any suffering for the animals. The hair is removed applying the cream for hair removal. For echocardiography, the mouse is picked up in the palm of one hand. Pre-warmed echo transmission gel is applied to the hairless chest. The transducer is applied on the chest. Annulus dimensions were obtained in the parasternal long axis view during systole for semilunar valves, and the apical four-chamber view during diastole for atrioventricular

valves. The aortic root measurements were obtained in a modified parasternal long axis view during diastole. Doppler interrogation was performed on the atrioventricular valve inflow in the apical four-chamber view, and semilunar valve outflow in the parasternal long axis view to assess for stenosis. A modified parasternal long axis view was required in some cases to ensure ascertainment of the maximum velocity. Cardiac chamber dimensions were measured, and ventricular function were assessed from two-dimensional directed M-mode echocardiographic images obtained from the parasternal short axis view. Doppler images were obtained from the apical four chamber view in accordance with consensus guidelines. All measurements were obtained in triplicate and averaged.

3.6 Wheat germ agglutinin (WGA) and histoenzymatic staining

Whole hearts isolated from mice of 4, 6, 12 and 18 months of age (HIPK2^{-/-}, n=5 and WT, n=5) were fixed overnight in 4% aqueous buffered formalin, and processed for paraffin embedding. Coronal sections (10 µm thick) containing both right and left ventricles were processed. Wheat Germ Agglutinin Alexa Fluor® 488 Conjugate (WGA) was performed. WGA selectively binds to N-acetylglucosamine and N-acetylneuraminic acid (sialic acid) residues in eukaryotic cells. The slices were first deparaffinized and then rehydrated with ethanol at decreasing concentrations. The slices were treated with Proteinase K, and then with Triton 1%. WGA were applied on the slices and quantified under fluorescent microscopy. Sequential sections from each heart were stained with haematoxylin and eosin (H&E) (Sigma-Aldrich), nicotinamide adenine dinucleotide (NADH) and cytochrome oxidase (COX).

Histological analysis of lungs and thyroid from WT and DKO at P1 by hematoxylin and eosin staining were performed. The antibody used were: anti-PAX8 (Amendola et al. 2005); anti-FOXE1 (Dathan et al. 2002); anti-Thyroglobulin rabbit polyclonal antibody (Dako). The secondary antibodies used were: goat anti-rat IgG polyclonal antibody conjugated to horseradish peroxidase (HRP) (GtxRt-003-DHRPX, ImmunoReagents, Inc).

All sections were examined under light microscope (Leitz, DIAPLAN), and images were acquired with a digital camera (Digital JVC, TK-C1380).

3.7 Fluorescence microscopy

Hearts from WT and HIPK2-KO mice were included in Optimal Cutting Temperature (OCT), quickly frozen to reduce ice crystal formation and minimize morphological damage, and 7 μm slices were obtained through transverse cut. Immunofluorescence assays were carried out on heart cryosections. Tissue slices were permeabilized with Triton 0,2% for 5 minutes, and blocked for 1 hour in BSA 2% and FBS 10% in phosphate-buffered saline (PBS) solution. Slices from WT and KO mice were stained with LC3 antibody (1:100, 0231-100/LC3-5F10, nanoTools, Teningen, Germany) and p62/SQSTM1 antibody (1:100, PM045, MBL Medical & biological laboratories CO., LTD) for 3 hours in the dark at room temperature. Primary antibodies were detected with Alexa-488 or Alexa-546 (Life Technologies, Camarillo, CA, USA) conjugated secondary antibodies. Nuclei were stained with DRAQ5 Fluorescent Probe Solution (1:1000 Cell Signaling Technology). Images were collected using a laser scanning microscope (LSM 510 META, Carl Zeiss Microimaging, Inc., Thornwood, NY, USA) equipped with a Plan Apo 63 \times oil-immersion (NA 1.4) objective lens. Quantification and morphometric analyses and co-localization analysis were carried out using LSM 510 software and the drawing tool was used to measure the relative dimensions and cell area.

3.8 Statistical analysis

Data are expressed as means \pm standard deviation (SD). Statistical significance between groups was assessed by Student's *t* test. For all analyses, a minimum value of $p < 0.05$ was considered significant.

4. RESULTS

4.1 Loss of HIPK2 induces cardiac dysfunction in mice

Previous observations have suggested a protective role of HIPK2 in cardiac function. Therefore, in order to study the *in vivo* role of HIPK2, we used the HIPK2-KO mouse model. To investigate whether HIPK2-KO mice develop cardiac defects, transthoracic echocardiography was performed on groups of 15 mice both WT and KO at 4 and 12 months of age. A significant reduction in percentage of left ventricular fractional shortening (LVFS%) was observed in 12-month old HIPK2-KO mice compared to age-matched WT, whereas no differences were detected at 4 months of age (Fig. 7A). Moreover, a significant increase in the heart weight (HW) to body weight (BW) ratio (HW/BW) was detected in HIPK2-KO mice with respect to WT mice from 12 months of age (Fig. 7B). As shown in figure 7C, we have observed a morphology of whole hearts of WT and HIPK2-KO mice at 12 months of age. In addition HIPK2-KO mice show smaller body size than WT counterparts (Fig. 7D). Collectively these data indicate that HIPK2-KO mice do not display early cardiac alterations, while significant reduction in systolic function can be detected in the middle-old mice.

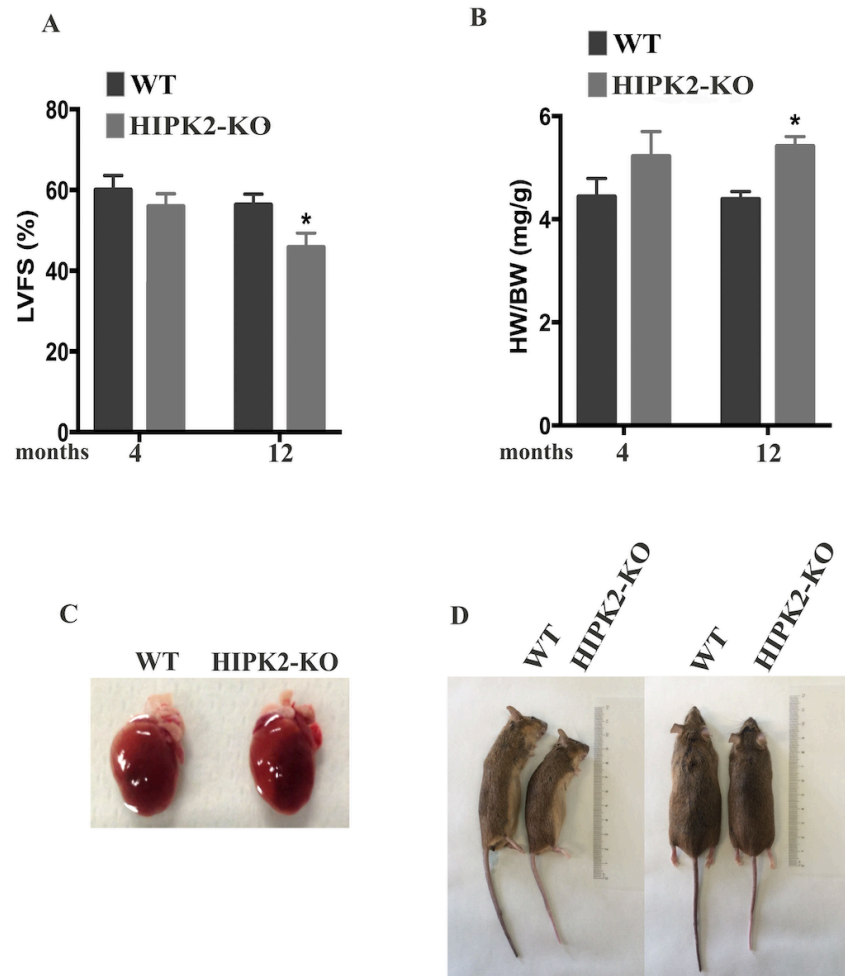
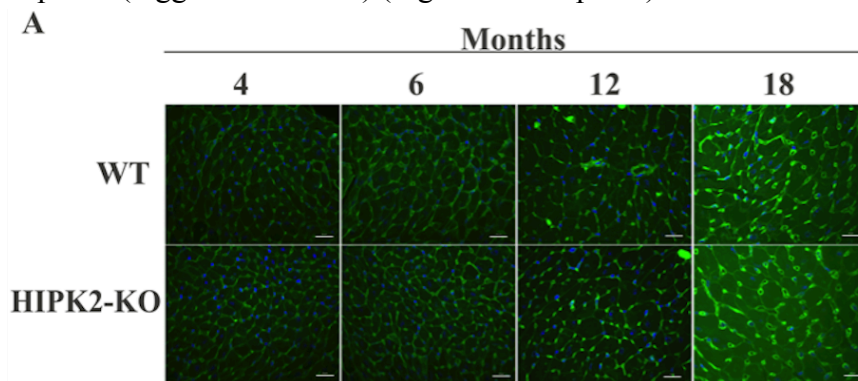


Figure 7. Echocardiographic and morphometric analysis of HIPK2-KO mice. **A** Bar graphs of % left ventricular fractional shortening (LVFS%) of WT and HIPK2-KO mice at 4 and 12 months of age (* $p < 0.05$). **B** Bar graphs showing heart weight to body weight ratio (HW/BW) in WT and HIPK2-KO mice at 4 and 12 months of age (* $p < 0.05$). **C** Representative morphology of whole hearts of WT and HIPK2-KO mice at 12 months of age. **D** Representative images of WT and HIPK2-KO mice at 12 months of age. The same mice are shown in two different positions: lateral and prone positions.

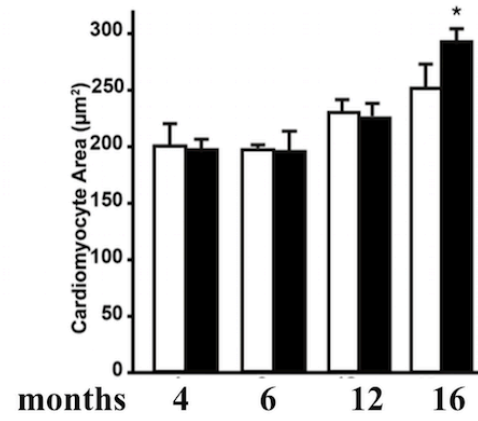
4.2 Loss of *HIPK2* induces an increase of the size of cardiomyocytes, cardiac inflammation and fibrosis

In order to characterize the heart morphology of *HIPK2*-KO mice, an histological analysis of the myocardium was performed by wheat germ agglutinin (WGA) staining of cardiac sections at different age (4, 6, 12, 18 months). As shown in figure 8A and 8B, cross-sectional area of cardiomyocytes from *HIPK2*-KO was significantly increased at 18 months of age compared to WT, whereas no differences were detected in younger mice. These data suggest that loss of *HIPK2* induces an age-dependent hypertrophy of cardiomyocytes in *HIPK2*-KO mice.

To better characterize the phenotype, we performed morphologic and histoenzymatic staining of cardiac muscle sections. Hematoxylin and eosin (H&E) was performed to evaluate heart morphology, while cytochrome oxidase (COX) and nicotinamide adenine dinucleotide (NADH) and stainings were performed to evaluate mitochondrial activity. H&E revealed a mild inflammatory infiltrate of lymphocytes in myocardium and a moderate fibrosis in *HIPK2*-KO mice at 18 months compared to WT controls (Fig. 8C upper panel). Moreover, COX staining revealed an overall normal mitochondrial activity, but several negative or partially negative fibers for COX activity were observed in *HIPK2*-KO mice (Fig. 8C middle panel). NADH staining showed several fibers with subsarcolemmal positive deposits (ragged blue fibers) (Fig. 8C lower panel).



B



C

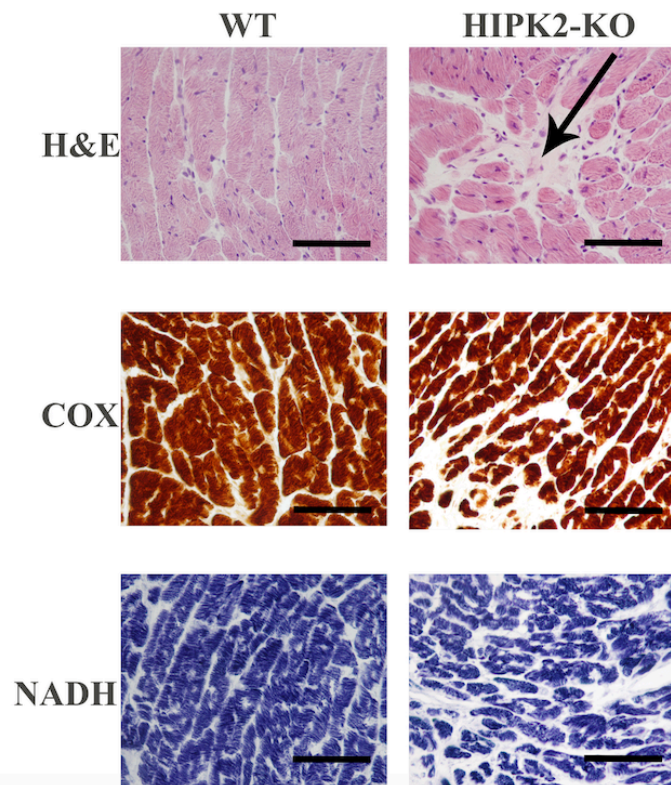


Figure 8. Histological analysis of the size of cardiomyocytes, inflammation and fibrosis in HIPK2-KO mice. **A** Representative images of WGA staining of sections from WT and HIPK2-KO mice at 4 up to 18 months of age. Scale bar= 60 μ m. **B** Quantification of cross sectional area of cardiomyocytes in the different experimental groups (*p < 0.05 vs. 4 months HIPK2^{-/-}, n=4 hearts/groups). **C** Representative H&E, COX and NADH staining of LV sections from WT and HIPK2-KO mice at 18 months of age (40x magnification); scale bar= 100 μ m. Arrow indicates fibrosis area.

4.3 Expression levels of cardiac failure markers are increased in HIPK2-KO mice

The above results clearly indicate that HIPK2-KO mice display alterations of heart. To assess whether morphological alterations are associated with changes in expression of molecular markers of cardiac failure and dysfunction, quantitative PCRs (qRT-PCR) for ANP, BNP and β -MHC were performed on cardiac apex of LV samples from WT and HIPK2-KO mice at 12 months. The mammalian heart expresses two closely related natriuretic peptide (NP) hormones, ANP and BNP. Plasma levels of BNP are used as diagnostic and prognostic markers for hypertrophy and heart failure (HF), and both ANP and BNP are widely used in biomedical research to assess the hypertrophic response.

As shown in figure 9, a significant increase of ANP, BNP and β -MHC expression was observed in HIPK2-KO mice.

Overall, these results are consistent with the cardiac dysfunctions observed by echocardiography and histology, and demonstrate that HIPK2 loss causes myocardial alterations leading to cardiac failure.

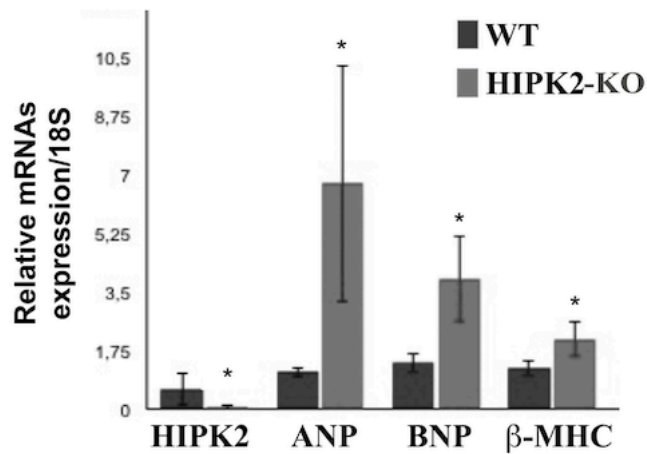


Figure 9. qRT-PCR analysis of cardiac failure markers in HIPK2-KO mice. RNA extracted from cardiac apex of LV samples of WT and HIPK2-KO at 12 months of age have been analyzed by qRT-PCR for ANP, BNP and β -MHC expression levels. The 18S ribosomal RNA housekeeping gene was used for normalization (* $p < 0.05$).

4.4 Altered autophagic pathway in HIPK2-KO mice

The presence of sarcoplasmic red deposits in the myocardium of HIPK2-KO mice may be attributable to autophagic vacuoles therefore, we evaluated the expression levels of p62/SQSTM1, an autophagic marker responsible for the addressing proteins to the autophagosomes. Immunofluorescence (IF) of heart cryosections of cardiomyocytes of WT and HIPK2-KO at 18 months of age, revealed an increased number of p62/SQSTM1 positive structures in HIPK2-KO mice (Fig. 10A). Consistently, levels of p62/SQSTM1 were increased in HIPK2-KO mice compared to WT mice at 12 months of age, as shown by Western blotting analysis (Fig. 10B). These data indicate that the loss of HIPK2 induces an alteration of the autophagic pathway in mice.

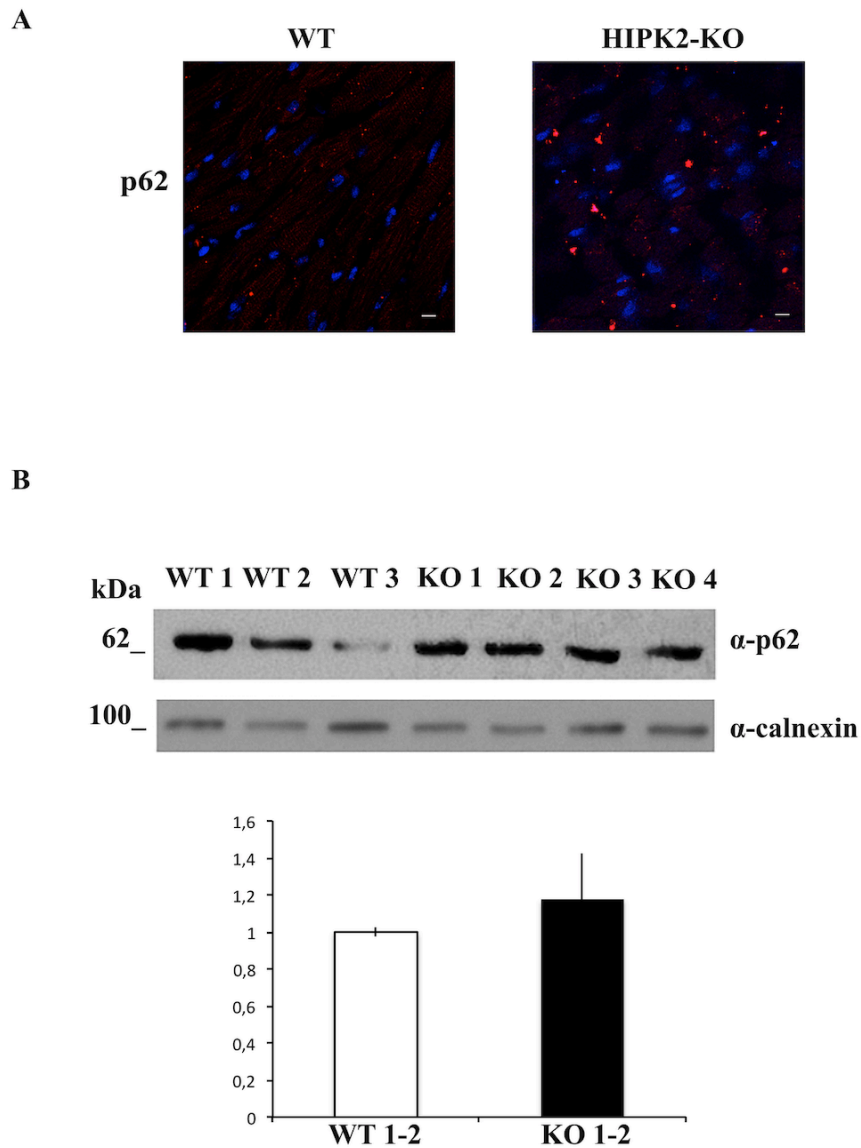


Figure 10. Evaluation of p62/SQSTM1 in HIPK2-KO mice. **A** Representative immunofluorescence images of heart cryosections of WT and HIPK2-KO mice at 18 months of age stained with p62/SQSTM1 antibody. Scale bar= 12 μ m. **B** Upper panel: Immunoblot detection of p62/SQSTM1 from lysates extracted from WT and HIPK2-KO heart sections of mice at 12 months of age. Calnexin was used as loading control. The molecular weight of

protein markers is indicated. The quantification of Western blotting is shown in lower panel.

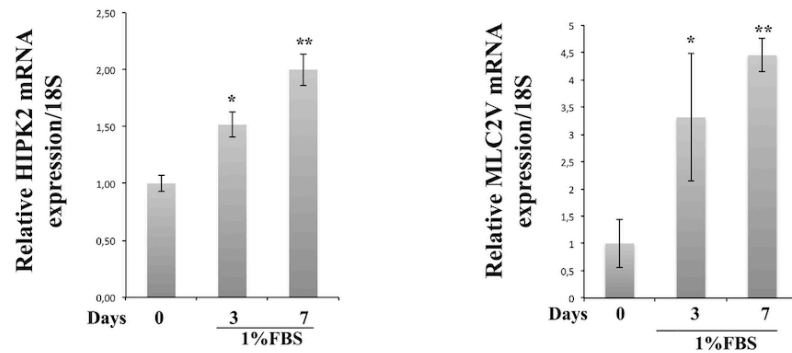
4.5 HIPK2 protein levels increase during differentiation of cardiomyoblasts

The above described data suggest a role of HIPK2 protein in cardiac homeostasis. To confirm this hypothesis, firstly we evaluated HIPK2 expression levels during cardiomyocyte differentiation *in vitro*. As a model system, we used the H9C2 rat cardiomyoblasts, which have been extensively characterized. H9C2 cells were cultured in DMEM. For their differentiation, they were initially grown with supplement of 10% FBS DMEM low glucose (1gr/l) for 3 days and switched to differentiation medium (1% FBS DMEM low glucose 1gr/l) for seven days (Comelli et al. 2011).

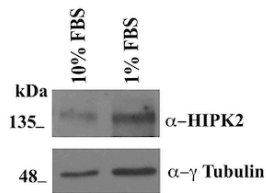
To evaluate if HIPK2 expression changes during the differentiation of H9C2 cells, I performed RNA extraction from rat cardiomyoblasts at day zero and from cardiomyocytes at days three and seven of differentiation. qRT-PCR analysis, performed using as control the differentiation marker ventricular myosin light chain 2 (MLC2V), showed that the endogenous HIPK2 is expressed at basal levels in cardiomyoblasts (day zero) and increases in cardiomyocytes after three and seven days of treatment with the differentiating medium (Fig. 11A). In parallel, western blot analysis performed on total cellular extracts at day zero and at day seven showed an increase of HIPK2 protein level (Fig. 11B). Moreover, we asked whether HIPK2 gene expression levels would change upon hypertrophic stimulus. In fact, it is known that cardiac hypertrophy is caused by an increased glucose uptake into the cardiac myocytes that determines a high glucose-mediated oxidative stress into the cardiomyocytes (Kagaya et al. 1990). This increased glucose uptake is mostly due to an imbalance of the translocation of GLUT1 and GLUT4 glucose transporters from intracellular membranes to the cell surface of the myocytes with a GLUT1/GLUT4 ratio favoring GLUT1 (Slot et al. 1991). On this basis, to induce hypertrophy, after 7 days of culture in differentiation conditions with DMEM 1% FBS 1gr/l glucose, H9C2 cells were treated for 24 hours with DMEM 1% FBS 4gr/l glucose. Interestingly, the hypertrophic stimulus induces a decrease in HIPK2 expression (Fig. 11C and 11D). These results strongly suggest that

HIPK2 could exert a protective role against induced cardiac hypertrophy.

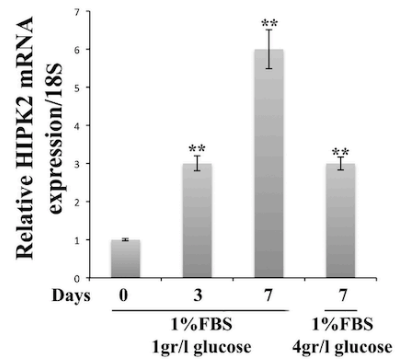
A



B



C



D

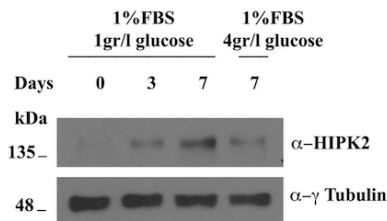
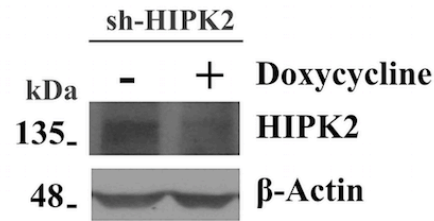


Figure 11. HIPK2 expression during cardiac differentiation. A RNAs extracted from H9C2 cells at different days were analyzed by qRT-PCR for HIPK2 and MLC2V expression levels. The 18S ribosomal RNA housekeeping gene was used for normalization (* $p < 0.05$; ** $p < 0.01$). B Protein extracted from H9C2 at 0 and 7 days were analyzed by Western blotting for HIPK2 protein expression.

Anti- γ -tubulin was used as loading control. **C** HIPK2 mRNA levels in H9C2 undifferentiated, differentiated and differentiated treated with an hypertrophic stimuli, the glucose, as measured by qRT-PCR. The amount of HIPK2 mRNA was normalized with respect to the amount of 18S ribosomal RNA housekeeping gene (* $p < 0.05$; ** $p < 0.01$). **D** Immunoblot detection of HIPK2 from lysates extracted from H9C2 cells treated with an hypertrophic stimuli, the glucose. To monitor equal loading of protein in the gel lanes, the blot was probed using anti- γ -tubulin antibody.

Finally, to evaluate the effect of HIPK2 down-regulation on cardiomyocyte differentiation, H9C2 cells were stably transfected with a plasmid coding for HIPK2 short hairpin RNA (shRNA). It interferes with the expression of HIPK2 and it is activated by doxycycline treatment. First, I used a pool clone to analyze HIPK2 protein expression. I focused on one pool showing about 50% of reduction of HIPK2 expression (Fig. 12A). I evaluated the expression levels of cardiac failure hallmarks, ANP, BNP and β -MHC upon HIPK2-knock-down by qRT-PCR analysis. As observed in figure 12B, a strong increase of ANP, BNP, and β -MHC mRNA levels were revealed confirming the evidence that HIPK2 may have a positive role in the induction of cardiac dysfunction.

A



B

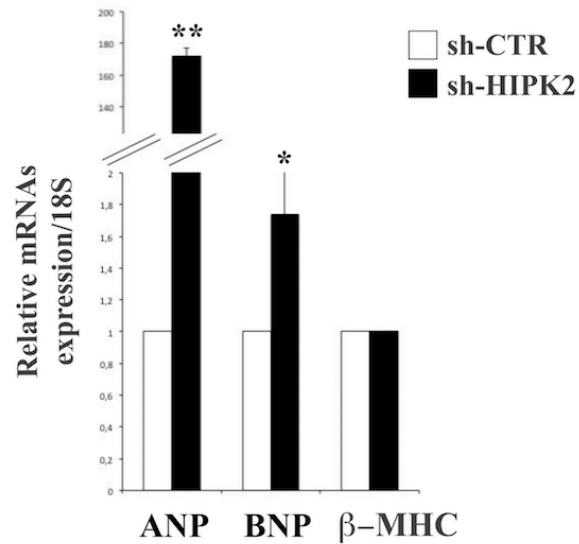


Figure 12. HIPK2 silencing promotes expression of cardiac failure markers in H9C2 cells. **A** Proteins extracted from H9C2 sh-HIPK2 were analyzed by Western blotting for HIPK2 protein expression. Anti- β actin was used as loading control. **B** RNA extracted from sh-HIPK2 H9C2 cells analyzed by qRT-PCR for

ANP, BNP and β -MHC expression levels. The 18S ribosomal RNA housekeeping gene was used for normalization (* p <0.05; ** p <0.01).

4.6 DKO mice show respiratory failure at birth and a decrease of expression of surfactant proteins in lung

As HIPK2 protein interacts with the architectural chromatin protein HMGA1 (Pierantoni et al. 2001), we have generated *Hmgal/Hipk2* double knock-out mice (DKO) to determine the functional role of *Hmgal* and *Hipk2* interaction *in vivo*. In collaboration with Prof. Fusco who has provided us single HMGA1-KO mice, we have crossed *Hmgal*-KO (A1-KO) mice and *Hipk2*-KO (HIPK2-KO) mice. The resulting double heterozygous were crossed to obtain the DKO mice. To verify the genotype of generated mice, DNA extracted from pieces of murine tails was amplified by PCR, using specific primers for WT and KO alleles of *Hmgal* and *Hipk2* genes. The amplified fragments were separated by electrophoresis on agarose gel to confirm the absence of HMGA1 and HIPK2 expression in DKO mice. We analyzed also, the phenotype of the DKO puppies. Observing the newborn mice, we have found that about 50% of DKO mice died within 12 hours after birth (P1). These mice appeared also smaller than the WT counterparts (Fig. 13A). Interestingly, also DKO mice that survive displayed smaller size and lower weight than their WT littermates (Fig. 13B).

Since DKO mice which died at P1 were cyanotic at birth and showed breathing difficulties, we hypothesized that the DKO could present lung abnormalities. To test this hypothesis, a post-mortem histological examination of DKO lungs was performed in comparison with WT mice at P1. Mice were sacrificed by CO₂ asphyxia by following university procedures approved by Animal Care Committee of the “Federico II”, University of Naples. To perform the experiments, lungs from WT and DKO mice were included in paraffin and 7 μ m sections were cut. By staining with hematoxylin and eosin, we observed that most of lungs from DKO mice were characterized by an immature pulmonary phenotype: these lungs presented collapsed immature sac-like alveoli (Fig. 13C) and unexpanded alveolar spaces containing abundant floccular eosinophilic material. This phenotype appears only in DKO lungs, whereas lungs from WT did not present abnormalities (Fig. 13D). Pulmonary surfactant is a surface-active lipoprotein complex

produced by type II alveolar cells: this complex is found in the fluid covering the alveolar surface of the lungs, where it plays several important roles. First of all, surfactant prevents alveolar collapse, and preserves bronchiolar patency during normal and forced respiration (Griese, 1999). It is well known that the absence of surfactant proteins results in lethal neonatal respiratory distress in both mice and human, and immunohistochemical studies demonstrated a lack of SP-A in infants dying before 48h of life (Markgraf et al. 1990). To test whether the HMGA1 and HIPK2 absence leads to an impaired expression of surfactant proteins, we performed quantitative RT-PCR (qRT-PCR) on total RNA extracted from WT and DKO lungs at P1. *Sp-A* and *Sp-B* expression was undetectable in all the DKO analyzed mice, and *Sp-C* expression was drastically reduced of about 58% compared to the WT mice (Fig. 13E). These results demonstrate that HMGA1 and HIPK2 proteins are required for the proper expression of surfactant proteins and, therefore, their cooperation is essential for the proper development of the lung.

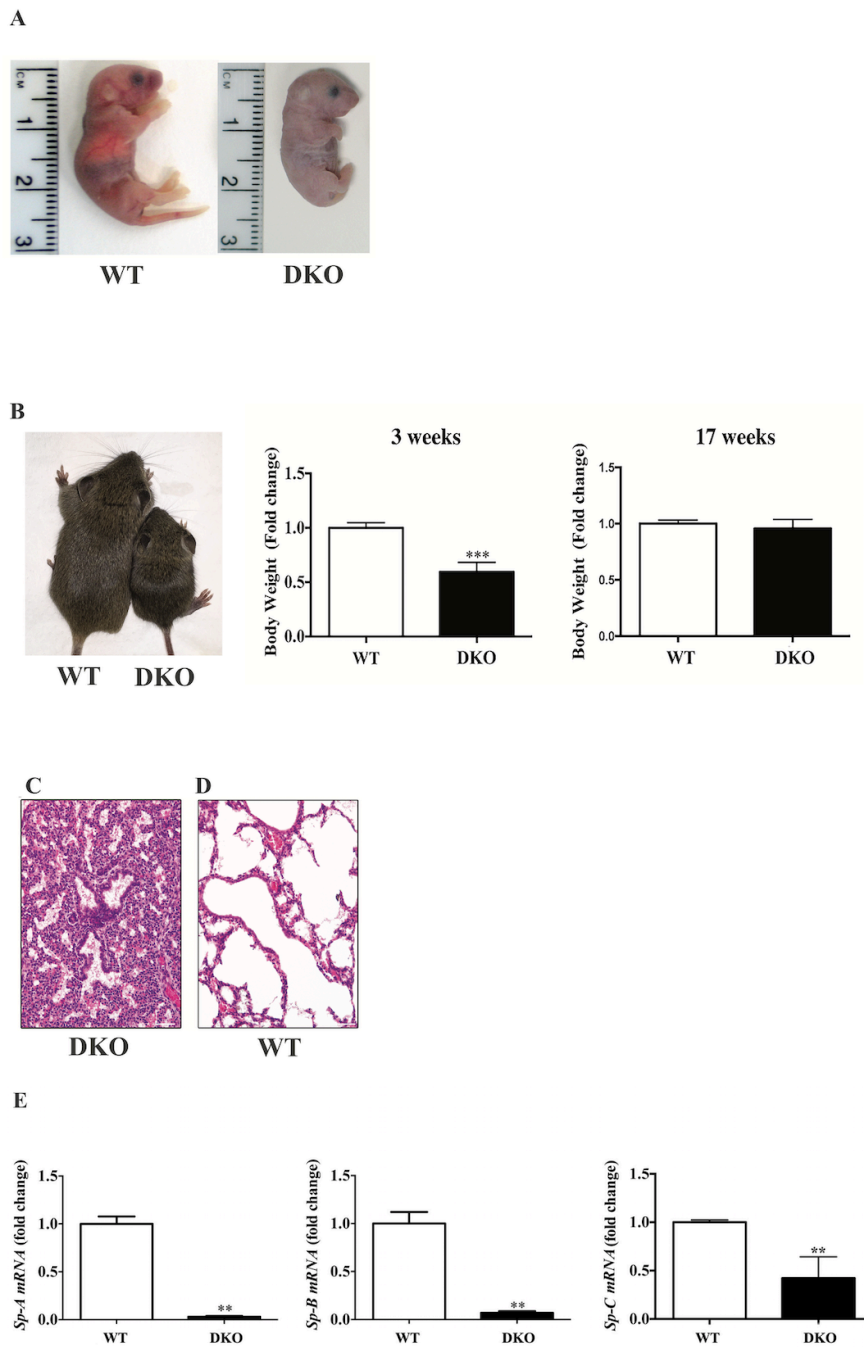


Figure 13. DKO mice display phenotypic alterations and a reduced surfactant expression levels in lungs. A Phenotypic differences between WT and DKO newborn puppies died at P1. **B**

DKO mice that survive appeared smaller and weight less than WT counterparts. In the left panel representative images of WT and DKO mice at 3 and 17 weeks of life (***) represent p value < 0.001 . **C-D** Histological analysis of WT and DKO lungs at P1 by hematoxylin and eosin staining (200x magnification). **E** RNAs extracted from WT and DKO lungs at P1 were analyzed by qRT-PCR for *Sp-A*, *Sp-B* and *Sp-C* expression. The actin expression level has been used for data normalization (** $p < 0.01$).

4.7 DKO mice display thyroid dysfunction

Since the DKO newborn puppies that survive at P1 appear smaller than the WT counterparts, we hypothesized a possible role of *Hmgal* and *Hipk2* interaction also in the thyroid function, because both lung and thyroid organs derive from the same embryonic layer, the endoderm. Moreover, during the perinatal period, adequate levels of thyroid hormones are critical to promote proper lung maturation and the proper development of lung and thyroid involves one common mediator, such as NKX2-1 (also called TTF-1) (Lazzaro et al. 1991). NKX2.1 is essential for brain, thyroid and lung development and differentiation (Minoo et al. 1995) and it regulates TG, TPO, and TSH gene expression (Civitareale et al. 1993; Francis-Lang et al. 1992). Furthermore, it is required for Sp-A, Sp-B, Sp-C and its absence causes lack of the lung parenchyma (De Felice et al. 2003; Kelly et al. 1996; Park et al. 2004).

To investigate this hypothesis, thyroid glands from DKO mice at P1 were compared to those from WT. Sections of neck containing the thyroid gland from WT and DKO mice at P1 were included in paraffin and 7 μ m slices were obtained. By H&E staining, we observed that thyroid from DKO was characterized by an irregular structure and the absence of colloid (Fig. 14A and 14B). Then, we asked whether differentiated thyroid follicular cells were present in DKO thyroid glands. It is known that differentiated thyroid follicular cells, are characterized by the coexpression of NKX2.1 (Lazzaro et al. 1991), FOXE1 (Zannini et al. 1997) and PAX8 (Plachov et al. 1990), which remain expressed after differentiation and are a hallmark of differentiated thyroid follicular cells. To analyze the expression of thyroid markers, immunohistochemistry analysis were performed on thyroid sections from DKO and WT mice at P1. FOXE1 and PAX8 protein levels were strongly reduced in thyroids

from DKO in comparison with WT as shown in figure 14 C-F.

Then, I performed IHC to evaluate the presence of colloid in DKO thyroids and qRT-PCR analysis to evaluate expression levels of late differentiation markers as thyroglobulin (*Tg*), thyroid peroxidase (*Tpo*) and thyrotropin receptor (*Tshr*). The expression of *Tpo* and *Tshr* mRNA were significantly reduced in DKO mice compared to the control mice at P1 (Fig. 14G). These data demonstrate that HMGA1 and HIPK2 have a key role in the thyroid function since their absence leads to a reduced expression of *Pax8* and *Foxe1* genes and this is responsible for the reduced amount of late thyroid markers TG, TPO and TSHr.

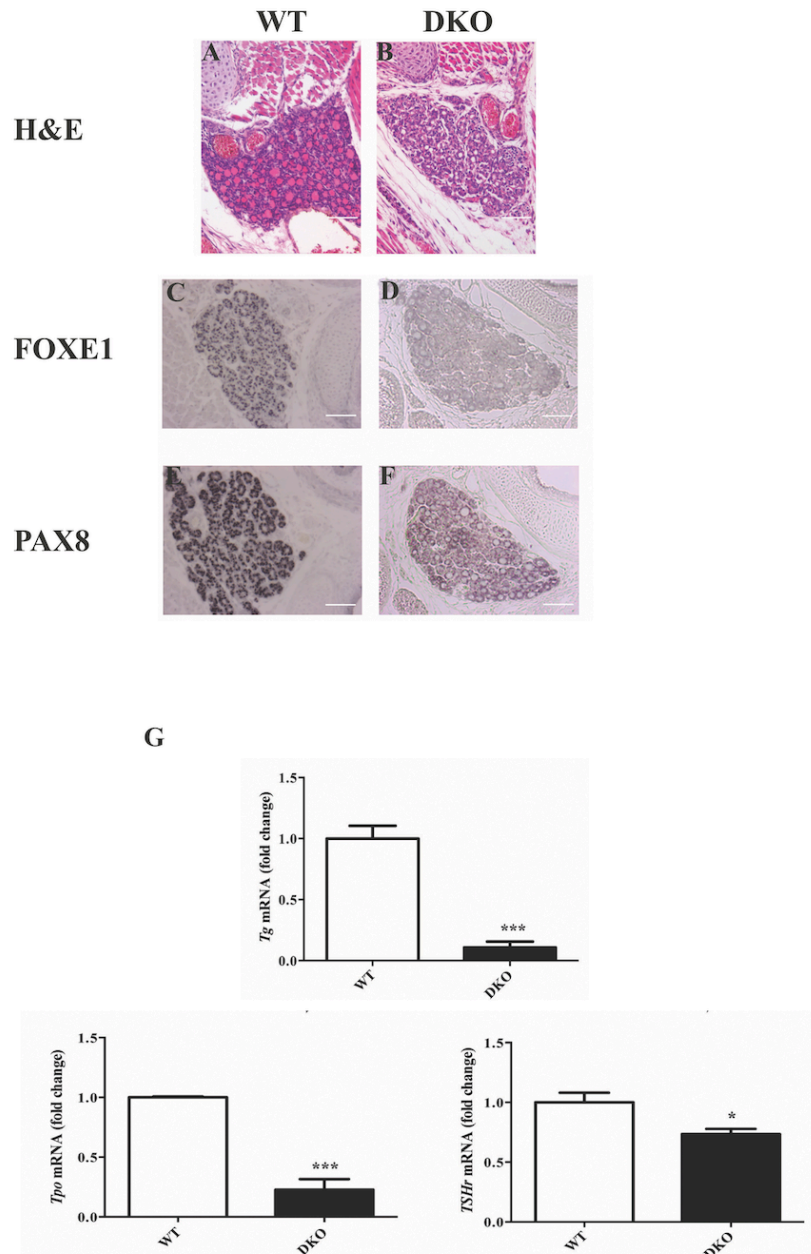


Figure 14. DKO leads to altered thyroid phenotype and impaired expression of thyroid markers in mice at P1. A-B Histological analysis of WT and DKO thyroid glands at P1 by hematoxylin and eosin staining revealed an altered phenotype in DKO mice (200x magnification). C-F IHC for FOXE1 and PAX8 expression were performed on WT and DKO sections of neck containing the thyroid

(20x magnification). **G** qRT-PCR on RNAs from WT and DKO mice at P1 was performed to evaluate the expression levels of *Tg*, *Tpo* and *Tshr* genes. Statistical differences are represented * $p < 0.05$; *** $p < 0.001$.

5. DISCUSSION AND CONCLUSIONS

During my PhD, I have investigated the *in vivo* role of the loss of HIPK2 taking advantage from *HIPK2*-KO mice. In particular from previous results I investigated the role of HIPK2 loss in cardiac homeostasis and the role of HMGA1/HIPK2 complex *in vivo*.

Echocardiographic analysis of *HIPK2*-KO mice has revealed a reduced cardiac function, evidenced by left ventricle fractional shortening (LVFS) at 12-months of age, whereas no differences with respect to WT mice have been detected at 4 months of age, indicating a significant reduction in systolic function in the adulthood (Fig. 7A). Indeed, expression levels of cardiac failure hallmarks, atrial and brain natriuretic peptides (ANP and BNP) and myosin heavy chain (β -MHC), were strongly increased (Fig. 9). Moreover, an histological analysis of the myocardium has revealed areas of fibrosis, mild inflammatory infiltrate and sarcoplasmic red deposits in cryosections of hearts from *HIPK2*-KO mice at 18 months of age (Fig. 8C). At cellular level, a lot of autophagic vacuoles p62/SQSTM1 positive have been observed (Fig. 10A). Therefore, the loss of HIPK2 induces cardiac dysfunction in mice that could be correlated to an altered autophagic pathway, indicating a critical role of HIPK2 in heart function. However, we did not find any variation in the expression levels of other autophagic proteins such as Microtubule-associated proteins 1A/1B light chain 3B (LC3) (data not shown).

The *HIPK2*-depleted cellular model of rat cardiomyoblasts H9C2 generated by us represents a tool to verify if *HIPK2* could play a role in cardiac differentiation. We observed that the endogenous *HIPK2* is expressed at basal levels in cardiomyoblasts and increases in cardiomyocytes at three and seven days of treatment with the differentiating medium (Fig. 11A) and the expression levels of cardiac failure hallmarks, such as ANP, BNP and β -MHC were strongly increased after *HIPK2* knock-down (Fig. 12B).

Altogether, these findings suggest that *HIPK2* is required to maintain normal cardiac homeostasis and that its deletion leads to cardiac dysfunction; indeed it has previously demonstrated the role of *HIPK2* in skeletal muscle cells differentiation (De la Vega et al. 2013). Moreover, a recent study has highlighted the protective role of *HIPK2* from pathological hypertrophy in cardiomyocytes (Guo et

al. Circulation 2018). In fact, Guo et al. have reported a decreased contractile function and the enlarged of left ventricle internal dimension in α MHC-Cre driven cardiomyocyte-specific HIPK2-KO mice. Furthermore, tamoxifen-induced deletion of HIPK2 in the adult mouse heart (KO, HIPK2^{flox/flox} α MHC-MerCreMer/) resulted in a decrease of heart function with a significant reduction of fractional shortening (FS) and ejection fraction (EF). This finding suggest that HIPK2 is required to mantain normal cardiac homeostasis and its deletion leads to cardiac dysfunction.

Cardiac dysfunction occurs in response to stresses from neurohumoral activation and hemodynamic overload. Persistent cardiac dysfunction usually progresses to chronic heart failure, which has a high mortality rate. Initially, the heart undergoes adaptive morphological changes that result in compensated hypertrophy to maintain cardiac output. Sustained hypertrophy is irreversible and inevitably results in decompensated heart failure (Li et al. 2018). Therefore, we also evaluated whether HIPK2 gene expression levels would change upon hypetrophic stimuly. Interestingly, the hypertrophic stimulus such as the glucose 4gr/l, induces a strong decrease in HIPK2 expression (Fig. 11C and 11D). These results strongly suggest that HIPK2 could exert a protective role against induced cardiac hypertrophy and that its loss could cause an hypertrophic phenotype of the heart.

Pathological left ventricular hypertrophy (LVH) is a hallmark feature of a number cardiovascular diseases and is strongly associated with increased risk of developing heart failure (Lewis et al. 1990). In response to stress, such as hypertension and pressure overload, several cellular modifications lead to cardiac remodeling (Burchfield et al. 2013). Despite the critical role of LVH in the development of cardiac dysfunction, the mechanisms underlying cardiac hypertrophy in response to pressure overload still remain not completely understood yet (Schiattarella et al. 2018). Therefore, further investigations of molecular mechanisms underlying cardiac hypertrophy, may allow to find new therapeutic approaches for this disease, involving new target molecules, including HIPK2.

As HIPK2 protein interacts with the architectural chromatin protein HMGA1 (Pierantoni et al. 2001), *Hmgal/Hipk2* double knock-out mice (DKO) have been generated in order to understand the functional role of *Hmgal* and *Hipk2* complex *in vivo*.

As discussed in the Introduction section, it is known that *Hipk2* gene is expressed from 15.5 days post coitum (d.p.c.) during embryogenesis and expressed in retinal cells, myoblasts and telencephalic neuroblasts during mouse embryogenesis. Conversely, it is ubiquitously expressed in murine and human adult tissues. Moreover, HIPK2 expression has been found down-regulated in breast and thyroid human carcinomas (Pierantoni et al. 2002). Instead, HMGA1, which is involved in embryogenesis, neoplastic transformation and adipocytic differentiation, is abundantly expressed in the all stages of embryonic development and begins to decline at 17-18 d.p.c., when *HIPK2* is expressed (Pierantoni et al. 2002).

Therefore in my PhD thesis, I have also investigated the functional role of HMGA1/HIPK2 interaction *in vivo* and the phenotype of HMGA1 and HIPK2 DKO mice. Surprisingly, 50% of HIPK2/HMGA1 DKO mice show perinatal lethality associated to respiratory distress. In fact, the maturation of the lung alveolar epithelium is delayed in the DKO mice, as indicated by post-mortem IHC analysis showing collapsed immature sac-like alveoli indicating a compromised lung development (Fig. 13A, 13C and 13D). HMGA1/HIPK2 proteins could be involved in the regulation of surfactant expression. Indeed, in the DKO mice, Sp-A and Sp-B expression was almost undetectable while Sp-C expression was strongly decreased with respect to their WT counterpart (Fig. 13E). This leads to a delay in the maturation of lung epithelial cells that we observed in DKO lungs. Altogether these data suggest that the lack or the strong reduction of surfactant expression caused by the loss of *Hmgal* and *Hipk2* expression is responsible for the death of DKO mice for respiratory distress. It is worth noting that mutations in the *Sp-B* gene are associated with fatal respiratory distress in the neonatal period, and mutations in the *Sp-C* gene are more commonly associated with interstitial lung disease in older infants, children, and adults (Wert et al. 2009). Moreover, it has been previously reported that HIPK2 regulate negatively the hypoxia-inducible factor-1 α (HIF-1 α) (Nardinocchi et al. 2009). HIF-1 α is responsible, among other transcription factors, for fetal lung development as it allows the fetus to quickly adapt to variation of oxygen concentrations. Indeed, lung-specific HIF-1 α KO leads to perinatal death in mice associated to impaired alveolar epithelial differentiation with consequent loss of surfactant protein expression (Saini et al. 2008). Therefore, the loss

of *Hipk2* expression may affect SP levels also by modulating HIF-1 α .

In addition, *Hmgal/Hipk2* DKO mice showed other phenotypic features associated to the development of the thyroid, in terms of lack of colloid accumulation in thyroid follicles and failure of the normal thyroid differentiation. Indeed, the autoptic examination of thyroid glands of DKO mice at P1 revealed thyroid abnormalities. The specific markers of thyroid differentiation, such as Tiroperoxidase (*Tpo*), Thyrotropin receptor (*Tshr*) and Thyroglobulin (*Tg*), are downregulated in DKO mice at P1, with the TG relocated mostly at the margins of the gland (Fig. 14A-F). The reduced expression of two thyroid specific transcription factors TTF2 and PAX8, that have been described as crucial for thyroid development and differentiation, likely accounts for this phenotype (Fig. 14G). Altogether these data suggest that lack of both *Hmgal* and *Hipk2* genes impairs the expression of PAX8 and FOXE1 in thyroid gland and, consequently, of thyroid differentiation markers, indicating that HMGA1/HIPK2 interaction is important also for thyroid development (Gerlini et al. Manuscript in submission). Moreover the association between lung and thyroid dysfunctions is not surprising, since both organs derive from the same embryonic layer, the endoderm.

In conclusion, the data obtained during my PhD thesis suggest a new putative role for the loss of HIPK2 in the pathogenesis of cardiac failure, and, in combination with the loss of HMGA1, of lung and thyroid dysfunction.

6. DECLARATION

The figures referred to experiments shown in this thesis could be included in several publications.

7. REFERENCES

- Anzilotti, S., Tornincasa, M., Gerlini, R., Conte, A., Brancaccio, P., Cuomo, O., Bianco, G., et al. 2015. "Genetic Ablation of Homeodomain-Interacting Protein Kinase 2 Selectively Induces Apoptosis of Cerebellar Purkinje Cells during Adulthood and Generates an Ataxic-like Phenotype." *Cell Death and Disease* 6 (12): e2004-11.
- Bennett, A.M. 1997. "Regulation of Distinct Stages of Skeletal Muscle Differentiation by Mitogen-Activated Protein Kinases." *Science* 278 (5341): 1288–1291.
- Burchfield, J.S., Min, X., and Hill, J.A. 2013. "Pathological Ventricular Remodeling." *Circulation* 128 (4): 388–400.
- Bustin, M., and Reeves, R. 1996. "High-Mobility-Group Chromosomal Proteins: Architectural Components That Facilitate Chromatin Function." *Progress in Nucleic Acid Research and Molecular Biology* 54: 35–100b.
- Chiappetta, G., Avantaggiato, V., Visconti, R., Fedele, M., Battista, S., Trapasso, F., Marciai, B.M., et al. 1996. "High level expression of the HMGI (Y) gene during embryonic development." *Oncogene* 5;13(11):2439-2446.
- Civitareale, D., Castelli, M.P., Falasca, P., and Saiardi, A. 1993. "Thyroid Transcription Factor 1 Activates the Promoter of the Thyrotropin Receptor Gene." *Molecular Endocrinology (Baltimore, Md.)* 7 (12): 1589–1595.
- Comelli, M., Domeis, R., Bisetto, E., Contin, M., Marchini, M., Ortolani, F., Tomasetti, L., et al. 2011. "Cardiac differentiation promotes mitochondria development and ameliorates oxidative capacity in H9c2 cardiomyoblasts." *Mitochondrion* 11(2): 315-326.
- D'Orazi, G., Cecchinelli, B., Bruno, T., Manni, I., Higashimoto, Y., Saito, S., Gostissa, M., et al. 2002. "Homeodomain-Interacting Protein Kinase-2 Phosphorylates P53 at Ser 46 and Mediates Apoptosis." *Nature Cell Biology* 4 (1): 11–19.
- De Felice, M., Silberschmidt, D., Di Lauro, R., Xu, Y., Wert, S.E., Weaver, T.E., Bachurski, C.J., et al. 2003. "TTF-1 Phosphorylation Is Required for Peripheral Lung Morphogenesis, Perinatal Survival, and Tissue-Specific Gene

- Expression.” *Journal of Biological Chemistry* 278 (37): 35574–35583.
- De La Vega, L., Hornung, J., Kremmer, E., Milanovic, M., and Schmitz, ML. 2013. “Homeodomain-Interacting Protein Kinase 2-Dependent Repression of Myogenic Differentiation Is Relieved by Its Caspase-Mediated Cleavage.” *Nucleic Acids Research* 41 (11): 5731–5745.
- Di Stefano, V., Soddu, S., Sacchi, A., and D’Orazi, G. 2005. “HIPK2 Contributes to PCAF-Mediated P53 Acetylation and Selective Transactivation of P21Waf1after Nonapoptotic DNA Damage.” *Oncogene* 24 (35): 5431–5442.
- Doxakis, E., Huang, EJ., and Davies, AM. 2004. “Homeodomain-Interacting Protein Kinase-2 Regulates Apoptosis in Developing Sensory and Sympathetic Neurons.” *Current Biology* 14 (19): 1761–1765.
- Fan, Y., Wang, N., Chuang, P., and He, JC. 2014. “Role of HIPK2 in kidney fibrosis.” *International Society of Nephrology* 4(1): 97–101.
- Federico, A., Forzati, F., Esposito, F., Arra, C., Palma, G., Barbieri, A., Palmieri, D., et al. 2014. “Hmga1/Hmga2 Double Knock-out Mice Display a ‘Superpygmy’ Phenotype.” *Biology Open* 3 (5): 372–378.
- Francis-Lang, H., Price, M., Polycarpou-Schwarz, M., and Di Lauro, R. 1992. “Cell-Type-Specific Expression of the Rat Thyroperoxidase Promoter Indicates Common Mechanisms for Thyroid-Specific Gene Expression.” *Molecular and Cellular Biology* 12 (2): 576–588.
- Fu, Y., Sun, X., and Lu, B., 2018. “HIPK3 Modulates Autophagy and HTT Protein Levels in Neuronal and Mouse Models of Huntington Disease.” *Autophagy* 14 (1): 169–710.
- Fusco, A., and Fedele, M. 2007. “Roles of HMGA Proteins in Cancer.” *Nature Reviews Cancer* 7 (12): 899–910.
- Glasser, S.W., Burhans, M. S., Korfhagen, T. R., Na, CL., Sly, PD., Ross, GF., Ikegami, M., et al. 2001. “Altered Stability of Pulmonary Surfactant in SP-C-Deficient Mice.” *Proceedings of the National Academy of Sciences* 98 (11): 6366–6371.
- Gresko, E., Roscic, A., Ritterhoff, S., Vichalkovski, A., Del Sal, G., and Schmitz, ML. 2006. “Autoregulatory Control of the P53 Response by Caspase-Mediated Processing of HIPK2.” *EMBO*

- Journal* 25 (9): 1883–1894.
- Griese, M. 1999. “Pulmonary Surfactant in Health and Human Lung Diseases: State of the Art.” *The European Respiratory Journal* 13 (6): 1455–1476.
- Guo, Y., Sui, J., Zhanh, Q., Barnett, J., Force, T., Lal, H., 2018. "Abstract18728: Loss of Homeodomain-Interacting Protein Kinase 2 in Cardiomyocytes Leads to Cardiac Dysfunction." *Circulation*.
- Hailemariam, K., Iwasaki, K., Huang, BW., Sakamoto, K., and Tsuji, Y. 2010. “Transcriptional Regulation of Ferritin and Antioxidant Genes by HIPK2 under Genotoxic Stress.” *Journal of Cell Science* 123 (22): 3863–3871.
- He, P., Yu, ZJ., Sun, CY., Jiao, SJ., and Jiang, HQ. 2017. “Knockdown of HIPK2 Attenuates the Pro-Fibrogenic Response of Hepatic Stellate Cells Induced by TGF-B1.” *Biomedicine and Pharmacotherapy* 85: 575–581.
- He, Q., Shi, J., Sun, H., An, J., Huang, Y., and M Sheikh, S. 2010. “Characterization of Human Homeodomain-Interacting Protein Kinase 4 (HIPK4) as a Unique Member of the HIPK Family.” *Molecular and Cellular Pharmacology* 2 (2): 61–68.
- Hofmann, TG., Jaffray, E., Stollberg, N., Hay, RT., and Will, H. 2005. “Regulation of Homeodomain-Interacting Protein Kinase 2 (HIPK2) Effector Function through Dynamic Small Ubiquitin-Related Modifier-1 (SUMO-1) Modification.” *Journal of Biological Chemistry* 280 (32): 29224–29232.
- Hofmann, TG., Möller, A., Sirma, H., Zentgraf, H., Taya, Y., Dröge, W., Will, H., and Schmitz, ML. 2002. “Regulation of P53 Activity by Its Interaction with Homeodomain-Interacting Protein Kinase-2.” *Nature Cell Biology* 4 (1): 1–10.
- Iacovelli, S., Ciuffini, L., Lazzari, C., Bracaglia, G., Rinaldo, C., Prodosmo, A., Bartolazzi, A., et al. 2009. “HIPK2 Is Involved in Cell Proliferation and Its Suppression Promotes Growth Arrest Independently of DNA Damage.” *Cell Proliferation* 42 (3): 373–384.
- Isono, K., Nemoto, K., Li, Y., Takada, Y., Suzuki, R., Katsuki, M., Nakagawara, A., et al. 2006. “Overlapping Roles for Homeodomain-Interacting Protein Kinases Hipk1 and Hipk2 in the Mediation of Cell Growth in Response to Morphogenetic and Genotoxic Signals.” *Molecular and Cellular Biology* 26

- (7): 2758–2571.
- Kagaya, Y., Kanno, Y., Takeyama, D., Ishide, N., Maruyama, Y., Takahashi, T., Ido, T., et al. 1990. “Effects of long-term pressure overload on regional myocardial glucose and free fatty acid uptake in rats. A quantitative autoradiographic study.” *Circulation* 81(4): 1353-1361.
- Kelly, SE., Bachurski, CJ., Burhans, MS., and Glasser, SW. 1996. “Transcription of the Lung-Specific Surfactant Protein C Gene Is Mediated by Thyroid Transcription Factor 1.” *J Biol Chem* 271 (12): 6881–6888.
- Kim, YH., Choi, CY., Lee, SJ., Conti, MA., and Kim, Y. 1998. “Homeodomain-Interacting Protein Kinases, a Novel Family of Co-Repressors for Homeodomain Transcription Factors.” *Journal of Biological Chemistry* 273 (40): 25875–25879.
- Kondo, S., Lu, Y., Debbas, M., Lin, AW., Sarosi, I., Itie, A., Wakeham, A., et al. 2003. “Characterization of Cells and Gene-Targeted Mice Deficient for the P53-Binding Kinase Homeodomain-Interacting Protein Kinase 1 (HIPK1).” *Proceedings of the National Academy of Sciences of the United States of America* 100 (9): 5431–5436.
- Kuwano, Y., Nishida, K., Akaike, Y., Kurokawa, K., Nishikawa, T., Masuda, K., and Rokutan, K. 2016. “Homeodomain-Interacting Protein Kinase-2: A Critical Regulator of the DNA Damage Response and the Epigenome.” *International Journal of Molecular Sciences* 17 (10).
- Larribère, L., Galach, M., Novak, D., Arévalo, K., Volz, HC., Stark, HJ., Boukamp, P., et al. 2017. “An RNAi Screen Reveals an Essential Role for HIPK4 in Human Skin Epithelial Differentiation from iPSCs.” *Stem Cell Reports* 9 (4): 1234–1245.
- Lazzaro, D., Price, M., De Felice, M., Di Lauro, R., and Di Lauro, R. 1991. “The Transcription Factor TTF-1 Is Expressed at the Onset of Thyroid and Lung Morphogenesis and in Restricted Regions of the Foetal Brain.” *Development (Cambridge, England)* 113 (4): 1093–1104.
- Lee, S., Shang, Y., Redmond, SA., Urisman, A., Tang, AA., Li, KH., Burlingame, AL., et al. 2016. “Activation of HIPK2 Promotes ER Stress-Mediated Neurodegeneration in Amyotrophic Lateral Sclerosis.” *Neuron* 91 (1): 41–55.

- Li, Y., Wang, Y., Zou, M., Chen, C., Chen, Y., Xue, R., Dong, Y., et al. 2018. "AMPK Blunts Chronic Heart Failure by Inhibiting Autophagy." *Bioscience Reports* 38 (4).
- Li, XL., Aray, Y., Harada, I., Shima, Y., Yoshida, H., Rokudai, S., et al. 2007. "Mutations of the HIPK2 gene in acute myeloid leukemia and myelodysplastic syndrome impair AML-1 and p53 mediated transcription." *Oncogene* 8;26(51): 7231-7239.
- Lombardi, LM., Zaghlula, M., Sztainberg, Y., Baker, SA., Klisch, TJ., Tang, AA., Huang, EJ., et al. 2017. "An RNA Interference Screen Identifies Druggable Regulators of MeCP2 Stability." *Science Translational Medicine* 9 (404).
- Mao, JH, Wu, D., Kim, IJ., Kang, HC., Wei, G., Climent, J., et al. 2011. "Hipk2 cooperates with p53 to suppress γ rayradiation-induced mouse thymic lymphoma." *Oncogene* 31: 1176-1180.
- Minoo, P., Hamdan,H., Bu, D., Warburton, D., Stepanik, P and Delemos, R. 1995. "TTF-1 Regulates Lung Epithelial Morphogenesis." *Developmental Biology* 172 (2): 694–698.
- Morrissey, EE., and Brigid L.M. Hogan. 2010. "Preparing for the First Breath: Genetic and Cellular Mechanisms in Lung Development." *Developmental Cell* 18 (1): 8–23.
- Nardinocchi, L., Puca, R., Sacchi, A., and D’Orazi, G. 2009. "Inhibition of HIF-1 α Activity by Homeodomain-Interacting Protein Kinase-2 Correlates with Sensitization of Chemoresistant Cells to Undergo Apoptosis." *Molecular Cancer* 8: 1–9.
- Nugent, MM., Lee, K., and He, JC. 2015. "HIPK2 Is a New Drug Target for Anti-Fibrosis Therapy in Kidney Disease." *Frontiers in Physiology* 6 (APR): 1–5.
- Paladino, S., Conte, A., Caggiano, R., Pierantoni, GM., and Faraonio, R. 2018. "Nrf2 Pathway in Age-Related Neurological Disorders: Insights into MicroRNAs." *Cellular Physiology and Biochemistry* 47 (5): 1951–1976.
- Park, KS., Whitsett, JA., Di Palma, T., Hong, JH., Yaffe, MB and Zannini, M. 2004. "TAZ Interacts with TTF-1 and Regulates Expression of Surfactant Protein-C." *Journal of Biological Chemistry* 279 (17): 17384–17390.
- Pierantoni, GM., Fedele, M., Pentimalli, F., Benvenuto, G., Pero, R., Viglietto, G., Santoro, M., et al. 2001. "High Mobility Group I (Y) Proteins Bind HIPK2, a Serine-Threonine Kinase Protein

- Which Inhibits Cell Growth.” *Oncogene* 20 (43): 6132–6141.
- Pierantoni, GM., Pentimalli, F., Fedele, M., Santoro, M., Fusco, A., Bulfone, A., Ballabio, A., et al. 2002. “The Homeodomain-Interacting Protein Kinase 2 Gene Is Expressed Late in Embryogenesis and Preferentially in Retina, Muscle, and Neural Tissues.” *Biochemical and Biophysical Research Communications* 290 (3): 942–947.
- Plachov, D., Chowdury, K., Walther, C., Simon, D., Guenet, JL., and Gruss, P. 1990. “Pax 8, a Murine Paired Box Gene Expressed in the Developing Excretory System and Thyroid Gland.” *Development* 110: 643–651.
- Puca, R., Nardinocchi, L., D'Orazi, G., 2008. "Regulation of vascular endothelial growth factor expression by HIPK2." *J Exp Clin Cancer Res* 27: 1-7.
- Reeves, R. 2010. “Nuclear Functions of the HMG Proteins.” *Biochimica et Biophysica Acta (BBA) - Gene Regulatory Mechanisms* 1799 (1–2): 3–14.
- Rinaldo, C., Moncada, A., Gradi, A., Ciuffini, L., D'Eliseo, D., Siepi, F., Prodosmo, A., et al. 2012. “HIPK2 Controls Cytokinesis and Prevents Tetraploidization by Phosphorylating Histone H2B at the Midbody.” *Molecular Cell* 47 (1): 87–98.
- Rinaldo, C., Prodosmo, A., Mancini, F., Iacovelli, S., Sacchi, A., Moretti, F., and Soddu, S. 2007. “MDM2-Regulated Degradation of HIPK2 Prevents P53Ser46 Phosphorylation and DNA Damage-Induced Apoptosis.” *Molecular Cell* 25 (5): 739–750.
- Rodriguez-Gil, A., Ritter, O., Hornung, J., Stekman, H., Kruger, M., Braun, T., Kremmer, E., et al. 2016. “HIPK Family Kinases Bind and Regulate the Function of the CCR4-NOT Complex.” *Molecular Biology of the Cell* 27 (12): 1969–1980.
- Roscic, A., Möller, A., Calzado, MA., Renner, F., Wimmer, VC., Gresko, E., Lüdi, KS., et al. 2006. “Phosphorylation-Dependent Control of Pc2 SUMO E3 Ligase Activity by Its Substrate Protein HIPK2.” *Molecular Cell* 24 (1): 77–89.
- Saini, Y., Harkema, JR., and Lapres, JJ. 2008. “HIF1 α Is Essential for Normal Intrauterine Differentiation of Alveolar Epithelium and Surfactant Production in the Newborn Lung of Mice.” *Journal of Biological Chemistry* 283 (48): 33650–33657.
- Schiattarella, GG., Boccella, N., Paolillo, R., Cattaneo, F., Trimarco,

- V., Franzone, A., D'Apice, S., et al. 2018. "Loss of Akap1 Exacerbates Pressure Overload-Induced Cardiac Hypertrophy and Heart Failure." *Frontiers in Physiology* 9: 1–11.
- Schiattarella, Gabriele G., and Hill, JA. 2015. "Inhibition of Hypertrophy Is a Good Therapeutic Strategy in Ventricular Pressure Overload." *Circulation* 131 (16): 1435–1447.
- Schiattarella, GG., Hill, TM., and Hill, JA. 2017. "Is Load-Induced Ventricular Hypertrophy Ever Compensatory?" *Circulation* 136 (14): 1273–1275.
- Shojima, N., Hara, K., Fujita, H., Horikoshi, M., Takahashi, N., Takamoto, I., Ohsugi, M. et al. 2012. "Depletion of Homeodomain-Interacting Protein Kinase 3 Impairs Insulin Secretion and Glucose Tolerance in Mice." *Diabetologia* 55 (12): 3318–3330.
- Siasos, G., Tsigkou, V., and Tousoulis, D. 2018. "Circulating MicroRNAs as Novel Biomarkers in Heart Failure." *Hellenic Journal of Cardiology*, 6–7.
- Slot, WJ., Geuze, HJ., Gigengack, S., James, DE., Lienhard, GE. 1991. "Translocation of the glucose transporter GLUT4 in cardiac myocytes of the rat." *PNAS* 88 (17): 7815-7819.
- Stanga, S., Lanni, C., Govoni, S., Uberti, D., D'Orazi, G., and Racchi, M. 2010. "Unfolded P53 in the Pathogenesis of Alzheimer's Disease: Is HIPK2 the Link?" *Aging* 2 (9): 545–554.
- Torrente, L., Sanchez, C., Moreno, R., Chowdhry, S., Cabello, P., Isono, K., Koseki, H., et al. 2017. "Crosstalk between NRF2 and HIPK2 Shapes Cytoprotective Responses." *Oncogene* 36 (44): 6204–6212.
- Wei, G., Ku, S., Ma, GK., Saito, S., Tang, AA., et al. 2007. "Hipk2 repress β catenin mediated transcription, epidermal stem cell expansion and skin tumorigenesis." *Proc Natl Acad Sci* 13040-13045.
- Wert, SE., Whitsett, JA., and Noguee, LM. 2009. "Genetic Disorders of Surfactant Dysfunction." *Pediatric and Developmental Pathology* 12 (4): 253–274.
- Whitsett, JA., and Glasser, SW. 1998. "Regulation of Surfactant Protein Gene Transcription." *Biochimica et Biophysica Acta* 1408 (2–3): 303–311.
- Whitsett, JA., and Alenghat, T. 2015. "Regulation of Surfactant

- Protein Gene Transcription.” *Nature Immunology* 16 (1): 27–35.
- Wiggins, AK., Wei, G., Doxakis, E., Wong, C., Tang, AA., Zang, K., Luo, EJ., et al. 2004. “Interaction of Brn3a and HIPK2 Mediates Transcriptional Repression of Sensory Neuron Survival.” *Journal of Cell Biology* 167 (2): 257–267.
- Yu, J., Deshmukh, H., Gutmann, Rj., Emnett, RJ., Rodriguez, FJ et al. 2009. "Alterations of BRAF and HIPK2 loci predominate in sporadic pilocytic astrocytoma." *Neurology* 1526-1531.
- Zannini, M., Avantaggiato, V., Biffali, E., Arnone, MI., Sato, K., Pischetola, M., Taylor, BA., et al. 1997. “TTF-2, a New Forkhead Protein, Shows a Temporal Expression in the Developing Thyroid Which Is Consistent with a Role in Controlling the Onset of Differentiation.” *EMBO Journal* 16 (11): 3185–3197.
- Zhang, J., Pho, V., Bonasera, SJ., Holzmann, J., Tang, AA., Hellmuth, J., Tang, S., et al. 2007. “Essential Function of HIPK2 in TGFβ-Dependent Survival of Midbrain Dopamine Neurons.” *Nature Neuroscience* 10 (1): 77–86.
- Zhang, Q., and Wang, Y. 2007. “Homeodomain-Interacting Protein Kinase-2 (HIPK2) Phosphorylates HMGA1a at Ser-35, Thr-52, and Thr-77 and Modulates Its DNA Binding Affinity.” *Journal of Proteome Research* 6 (12): 4711–4719.
- Zhang, Q., Yoshimatsu, Y., Hildebrand, J., Frisch, SM., and Goodman, RH. 2003. “Homeodomain Interacting Protein Kinase 2 Promotes Apoptosis by Downregulating the Transcriptional Corepressor CtBP.” *Cell* 115 (2): 177–186.
- Zhou, X., Benson, KF., Ashar, HR., and Chada, K. 1995. “Mutation Responsible for the Mouse Pygmy Phenotype in the Developmentally Regulated Factor HMGI-C.” *Nature*.

8. LIST OF PUBLICATIONS

1. **Cammarota F**, Fiscardi F, Esposito T, de Vita G, Salvatore M, Laukkanen MO. Clinical relevance of thyroid cell models in redox research. *Cancer Cell Int.* 2015 Dec 9; 15:113. doi: 10.1186/s12935-015-0264-3.
2. **Cammarota F**, Laukkanen MO. Mesenchymal Stem/Stromal Cells in Stromal Evolution and Cancer Progression. *Stem Cells Int.* 2016; 2016:4824573. doi: 10.1155/2016/4824573.
3. **Cammarota F**, De Vita G, Salvatore M and Laukkanen MO. Ras Oncogene Mediated Progressive Silencing of Extracellular Superoxide Superoxide Dismutase in Tumorigenesis. *BioMed Research International* 2015. doi: 10.1155/2015/780409.
4. Castellone MD, **Cammarota F**, Esposito T, Salvatore M, and Laukkanen MO. Extracellular Superoxide Dismutase Regulates the Expression of Ras Superfamily GTPase Regulatory Proteins GEFs, GAPs, and GDI. *Plos One* 2015 doi: 10.1371.
5. Gerlini R, Amendola E, Tornincasa M, Conte A, **Cammarota F**, Gentile C, Di Guida L, Paladino S, De Vita G, De Felice M, Fusco A and Pierantoni GM. Double knock-out of *Hmgal* and *Hipk2* genes causes perinatal death associated to respiratory distress and thyroid abnormalities in mice. Ready to submission on “Cell Death and Disease”.
6. **Cammarota F**, De Pasquale V, Schiattarella GG, Boccella N, Paciello O, De Biase D, Iacobellis F, Conte A, Zerillo L, Paladino S, Pavone LM, Pierantoni GM. HIPK2 genetic ablation induces cardiac dysfunction in mice. Ready to submission on “International Journal of Molecular Sciences”.